ACS BIO & MED CHEM Au
AN OPEN ACCESS JOURNAL OF THE AMERICAN CHEMICAL SOCIETY

pubs.acs.org/biomedchemau
Article

Fusing Peptide Epitopes for Advanced Multiplex Serological Testing for SARS-CoV-2 Antibody Detection

Ali H. Aldoukhi, Panayiotis Bilalis, Dana M. Alhattab, Alexander U. Valle-Pérez, Hepi H. Susapto, Rosario Pérez-Pedroza, Emiliano Backhoff-García, Sarah M. Alsawaf, Salwa Alshehri, Hattan Boshah, Abdulelah A. Alrashoudi, Waleed A. Aljabr, Manal Alaamery, May Alrashed, Rana M. Hasanato, Raed A. Farzan, Roua A. Alsubki, Manola Moretti, Malak S. Abedalthagafi, and Charlotte A. E. Hauser*

Cite This: ACS Bio Med Chem Au 2024, 4, 37−52

Read Online

ACCESS | Metrics & More | Article Recommendations | Supporting Information

ABSTRACT: The tragic COVID-19 pandemic, which has seen a total of 655 million cases worldwide and a death toll of over 6.6 million seems finally tailing off. Even so, new variants of severe acute respiratory syndrome coronavirus 2 (SARS-CoV-2) continue to arise, the severity of which cannot be predicted in advance. This is concerning for the maintenance and stability of public health, since immune evasion and increased transmissibility may arise. Therefore, it is crucial to continue monitoring antibody responses to SARS-CoV-2 in the general population. As a complement to polymerase chain reaction tests, multiplex immunoassays are elegant tools that use individual protein or peptide antigens simultaneously to provide a high level of sensitivity and specificity. To further improve these aspects of SARS-CoV-2 antibody detection, as well as accuracy, we have developed an advanced serological peptide-based multiplex assay using antigen-fused peptide epitopes derived from both the spike and the nucleocapsid proteins. The significance of the epitopes selected for antibody detection has been verified by in silico molecular docking simulations between the peptide epitopes and reported SARS-CoV-2 antibodies. Peptides can be more easily and quickly modified and synthesized than full length proteins and can, therefore, be used in a more cost-effective manner. Three different fusion-epitope peptides (FEPs) were synthesized and tested by enzyme-linked immunosorbent assay (ELISA). A total of 145 blood serum samples were used, compromising 110 COVID-19 serum samples from COVID-19 patients and 35 negative control serum samples taken from COVID-19-free individuals before the outbreak. Interestingly, our data demonstrate that the sensitivity, specificity, and accuracy of the results for the FEP antigens are higher than for single peptide epitopes or mixtures of single peptide epitopes. Our FEP concept can be applied to different multiplex immunoassays testing not only for SARS-CoV-2 but also for various other pathogens. A significantly improved peptide-based serological assay may support the development of commercial point-of-care tests, such as lateral-flow-assays.

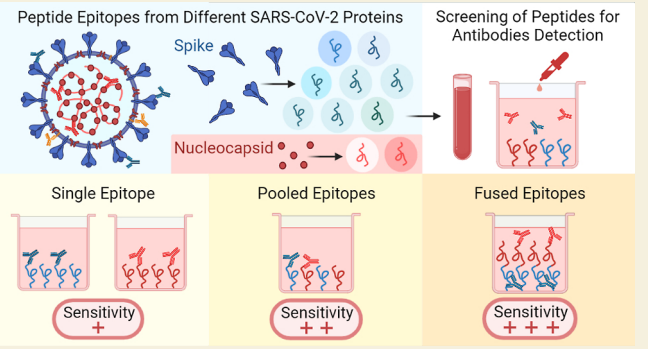

KEYWORDS: *SARS-CoV-2, COVID-19, peptide epitopes, ELISA, diagnostics*

INTRODUCTION

Severe acute respiratory syndrome corona virus 2 (SARS-CoV-2) is an RNA virus and the causative agent of COVID-19 (coronavirus disease 2019), which was first identified in December 2019.[1] The main antigenic part of the virus is the spike protein, a surface protein that facilitates viral entry into cells mainly through its interaction with the angiotensin-converting enzyme (ACE2) receptor.[2] The virus can be detected at the early stages of the disease by a polymerase chain reaction (PCR) test from the first day of the infection until approximately 21 days after the infection.[3] Early detection of the virus is a crucial step to isolate cases and limit the virus spread.[4] Antibodies against the viral surface proteins, including the spike and nucleocapsid proteins, play an essential role in the immune system fight mechanism and detection of immunized individuals.[3] IgG and IgM antibodies start to appear seven days after the disease onset, and their levels can be sustained in the blood for several months providing immunity against a second infection.[3] Early in the pandemic, detection of SARS-CoV_2 antibodies helped to contain and manage the pandemic by detecting people who have immunity

Received: February 4, 2023
Revised: July 29, 2023
Accepted: July 31, 2023
Published: August 30, 2023

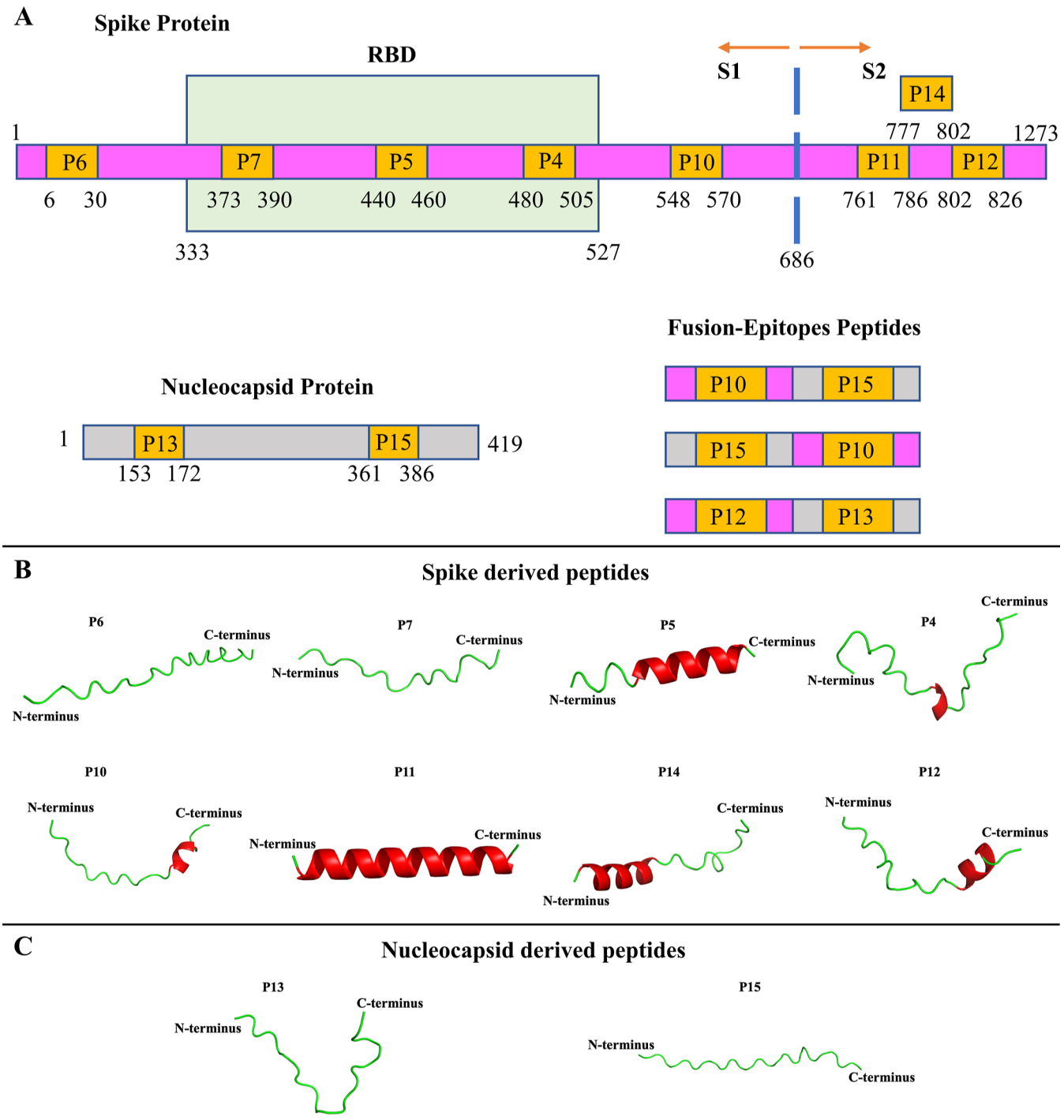

Figure 1. (A) Mapping of the synthesized peptides against the full spike and nucleocapsid protein sequences. AlphaFold 2 three-dimensional structure prediction for the (B) spike and (C) nucleocapsid-derived peptides. The peptide secondary structures are labeled in red (helix) and green (random coil), respectively (B,C).

against the virus.[5] Due to emerging new viral variants with the potential to evade the immune response, there is a continuous public health need for serological testing as an auxiliary method to screen for SARS-CoV-2 immunity in the general population.[6]

Serum antibodies are detected in clinical laboratories either using an enzyme-linked immunosorbent assay (ELISA) or a chemiluminescence immunoassay (CLIA).[7] In an ELISA, the antigen of interest, protein or peptide, is attached to a microtiter plate and used to detect antibodies in the samples that would bind to the antigen.[8] Peptide antigens have several advantages compared to protein antigens. First, peptides were reported to have better sensitivity when compared to proteins.[9] Second, producing proteins in their native form is challenging, which could negatively influence the consistency and outcomes of the test.[10] Lastly, peptide sequences can be readily changed to adapt any specific design requirements or change of viral protein sequence due to mutations in comparison to recombinant proteins.[11]

https://doi.org/10.1021/acsbiomedchemau.3c00010
ACS Bio Med Chem Au 2024, 4, 37−52

Table 1. List of the Synthesized Peptide Amino Acid Sequences[a]

peptide	amino acid sequence	protein	amino acid positions
P4	K(Biotin)CNGVEGFNCYFPLQSYGFQPTNGVGY	S	480−505
P5	K(Biotin)NLDSKVGGNYNYLYRLFRKSN	S	440−460
P6	K(Biotin)VLLPLVSSQCVNLTTRTQLPPAYTN	S	6−30
P7	K(Biotin)SFSTFKCYGVSPTKLNDL	S	373−390
P10	K(Biotin)GTGVLTESNKKFLPFQQFGRDIA	S	548−570
P11	K(Biotin)TQLNRALTGIAVEQDKNTQEVFAQVK	S	761−786
P12	K(Biotin)FSQILPDPSKPSKRSFIEDLLFNKV	S	802−826
P13	K(Biotin)NNAAIVLQLPQGTTLPKGFYA	N	153−172
P14	K(Biotin)NTQEVFAQVKQIYKTPPIKDFGGFNF	S	777−802
P15	K(Biotin)KTFPPTEPKKDKKKKADETQALPQRQ	N	361−386
FEP10-15	K(Biotin)-GTGVLTESNKKFLPFQQFGRDIA-SGSGS-KTFPPTEPKKDKKKKADETQALPQRQ	S−N	548−570(S)-361−386(N)
FEP15-10	K(Biotin)KTFPPTEPKKDKKKKADETQALPQRQ-SGSGS-GTGVLTESNKKFLPFQQFGRDIA	N−S	361−386(N)-548−570(S)
FEP12-13	K(Biotin)-FSQILPDPSKPSKRSFIEDLLFNKV-SGSGS-NNAAIVLQLPQGTTLPKGFYA	S−N	802−826(S)-153−172(N)

[a]LC−MS data are provided in Figures S1−S12.

Several studies have reported peptide epitopes from the SARS-CoV-2 surface proteins that can recognize serum antibodies from COVID-19 patients.[12−18] Various peptide sequences were identified in different studies and were found to have different sensitivity, specificity, and accuracy for antibody detection.[12−18] For example, Poh et al. screened overlapping peptide epitopes from the whole spike protein using ELISA to identify epitopes with reactivity against SARS-CoV-2 antibodies.[12] They found two epitopes from the spike protein (residues 553−570 and 809−826) that elicited a high response against SARS-CoV-2 antibodies. Li et al.[19] screened peptide epitopes spanning the entire length of the spike protein using microarray analysis and found similar epitopes to Poh et al.[12] and other additional epitopes that can be used for antibody detection. Even though some common peptide sequences were identified, the diagnostic performance for these sequences varied among the studies.[12,19]

A recent study assessed the antibody response of multiple patients to several peptide epitopes using ELISA.[17] They found that each peptide can detect antibodies from some serum samples but not the others. Thus, suggesting that a single peptide sequence might not be capable of detecting all patients with SARS-CoV-2 antibodies. One proposed way to resolve this issue is to use a pool or mixture of peptides when coating the microtiter plate to improve the sensitivity and specificity for detecting SARS-CoV-2 antibodies.[14,16,17]

Serological assays need to be highly sensitive and specific to detect the desired antibodies without false-negative or false-positive results. Therefore, several aspects need to be considered when developing a serological assay, including antigen selection.[20] Combining results from viral antigens has been shown to improve the sensitivity and specificity for antibody detection.[21] An alternative way to combine results from two antigens would be to synthesize one antigen with fused sequences from two different antigenic sites. This could improve the time and cost effectiveness of developing an immunoassay.

In this study, we aimed to improve the sensitivity, specificity, and accuracy of serological multiplex assays by fusing various peptide epitopes as a single antigen for the advanced detection of SARS-CoV-2 antibodies. For this purpose, selected peptide epitopes from the spike and nucleocapsid proteins with reported immunogenicity[12−14,22,23] were synthesized. All selected peptides were individually screened for the best performing peptide epitopes in terms of specificity and sensitivity for SARS-CoV-2 antibody detection. We identified four peptide epitopes out of 10 peptide candidates that reacted strongly with SARS-CoV-2 antibodies with the highest sensitivity level of 78%. The identified four peptides derived from both the spike and the nucleocapsid protein were chosen for the multiplex assay. They were tested as a mixture of two peptide epitopes or as a combined single epitope, by fusing the peptide sequences from the single epitopes. Interestingly, three of our designed fusion-epitope peptide (FEP) antigens showed significantly higher sensitivity, specificity, and accuracy for COVID-19 antibodies when compared with single peptide epitopes or mixtures of single peptide epitopes. Finally, we performed a simulation study of the docking between the peptide epitopes and the crystal structure of reported SARS-CoV-2 antibodies to demonstrate the docking efficiency between the peptide epitopes and antibodies. We improved the sensitivity level of antibody detection up to 88% when FEP was used. This data could help in understanding factors that can be utilized to improve the sensitivity, specificity, and accuracy of detecting SARS-CoV-2 antibodies. Furthermore, the result of this study could be used in developing peptide-based serological assays not only for SARS-CoV-2 but also for other diseases that require serological testing with high sensitivity and specificity.

RESULTS AND DISCUSSION

Patients Samples

A total of 145 samples were included in this study, consisting of 110 SARS-CoV-2 antibodies positive samples and 35 negative pre-COVID-19 samples. Pre-COVID-19 samples were de-identified and archived before November 2019. Regarding the positive samples, 95% were collected between July and September of 2020 and 5% were collected between January and February of 2021. Females and males represented 55 and 45%, respectively, of the sample with positive SARS-CoV-2 antibodies. The mean age of patients was 40 years (±13.4), and the mean duration between the positive PCR test and sample collection was 27.5 days (±13.3). This duration provided sufficient time for the immune system to develop detectable antibody levels in the blood after the infection.[3,24] All 110 positive samples were tested positive for SARS-SoV-2 antibodies using a commercial antibody test (Abbott COVID IgG test).

https://doi.org/10.1021/acsbiomedchemau.3c00010
ACS Bio Med Chem Au 2024, 4, 37−52

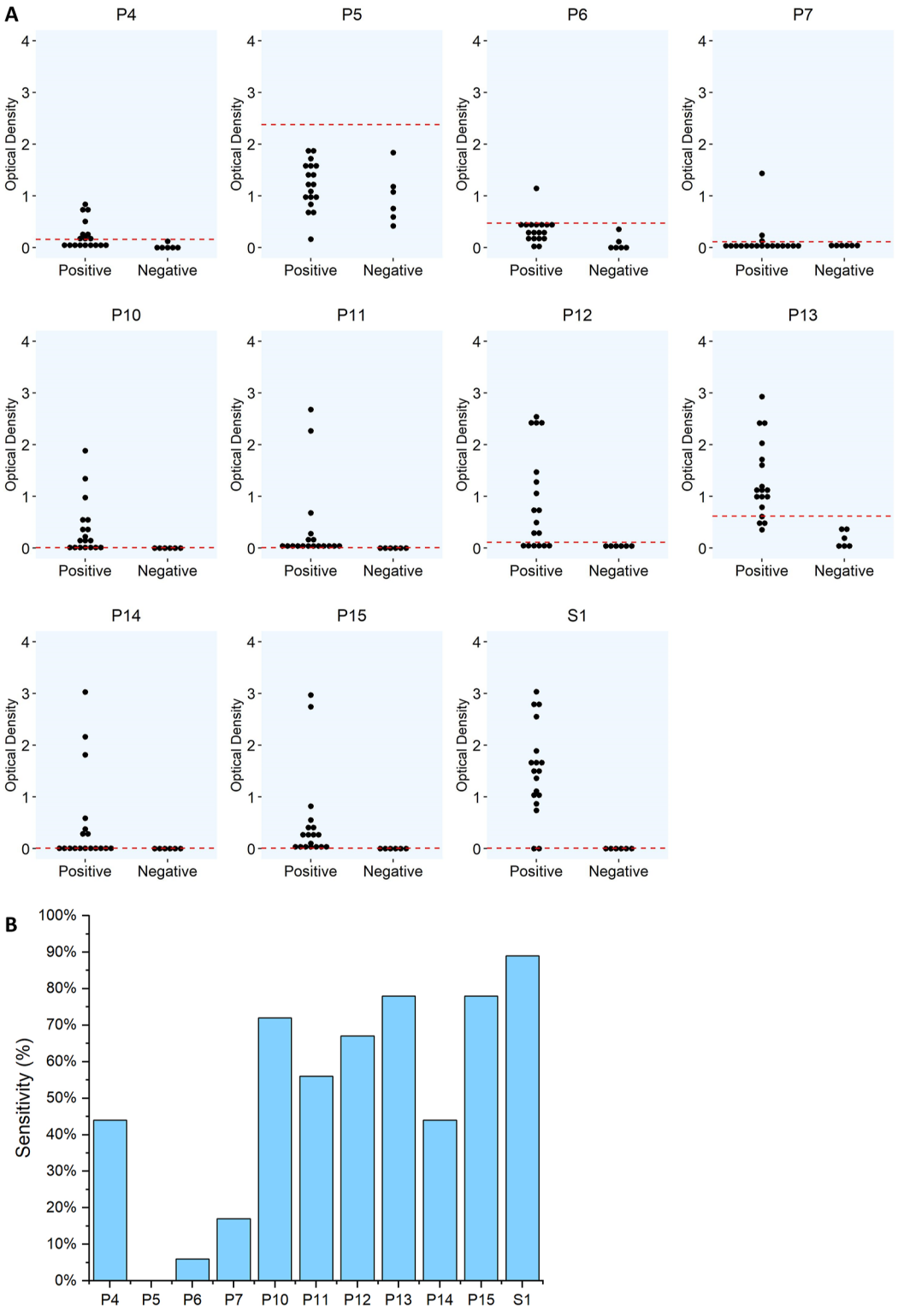

Figure 2. ELISA experiments screening all 18 SARS-CoV-2-positive samples and 6 pre-COVID-19 samples with single peptides (P4, P5, P10, P11, P12, P13, P14, and P15) and S1 subunit of the spike protein. Dashed line represents the threshold for each peptide (A). Sensitivity of the tested peptides in detecting SARS-CoV-2 antibodies from positive samples (B).

Screening All Antigens

In order to select those peptides with high sensitivity and specificity, we screened all 10 peptides (Figure 1, Table 1) with 24 random samples (18 positive samples, and six negative pre-COVID-19 samples). The differences in fluorescent signal intensity [optical density (OD) signal] between the different peptides and the S1 subunit of the spike protein are shown in Figure 2A. The threshold to determine positive and negative OD signals was calculated for each peptide; detailed information about how the threshold, sensitivity, and specificity were calculated can be found in the Experimental Section. The P4, P10, P12, P13, and P15 peptides and the

https://doi.org/10.1021/acsbiomedchemau.3c00010
ACS Bio Med Chem Au 2024, 4, 37−52

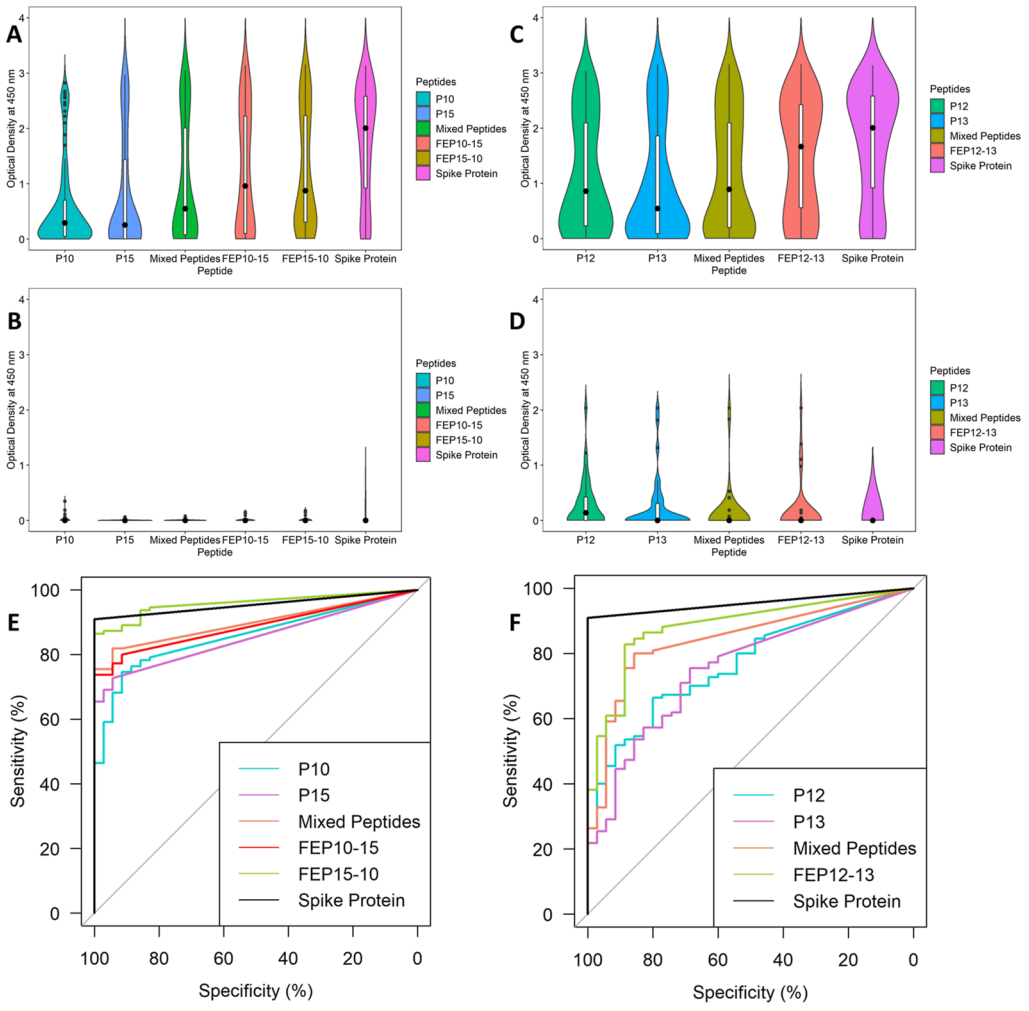

AUC (95% CI)	
P10	0.857 (0.801-0.910)
P15	0.852 (0.807-0.896)
Mixed Peptides	0.898 (0.854-0.936)
FEP10-15	0.887 (0.843-0.929)
FEP15-10	0.958 (0.927-0.982)
Spike Protein	0.954 (0.927-0.981)

AUC (95% CI)	
P12	0.767 (0.683-0.844)
P13	0.754 (0.668-0.835)
Mixed Peptides	0.843 (0.772-0.904)
FEP12-13	0.884 (0.823-0.937)
Spike Protein	0.954 (0.927-0.981)

Figure 3. OD results for P10, P15, mixed P10 + P15, FEP10-15, and FEP15-10 peptides when tested with (A) 110 positive samples and (B) 35 negative samples. OD results for P12, P13, mixed P12 + P13, and FEP12-13 peptides when tested with (C) 110 positive samples and (D) 35 negative samples. Spike protein control was included when testing all the samples. All peptides showed a statistically significant difference when comparing positive to negative pre-COVID-19 samples (p-value < 0.0001). Statistically significant difference between the groups is shown in the graph (***p < 0.001; **p < 0.01; *p < 0.05). Black dot in the middle of the box plot represents the median, and the violin plot was drawn with kernel density estimate. ROC curves (E) for P10, P15, mixed P10 + P15, FEP10-15, and FEP15-10 peptides and (F) for P12, P13, mixed P12 + P13, and FEP12-13 peptides showing the sensitivity and specificity for each peptide. AUC for each peptide is shown underneath each ROC figure.

Spike protein had a high number of positive samples that were above the threshold (Figure 2A). For the P5 peptide, the OD results were high for both positive and negative samples, which resulted in a high threshold cut-off value. The sensitivity of detecting SARS-CoV-2 antibodies was calculated for all the peptides and compared with the spike protein (Figure 2B). The highest sensitivity was 78% for nucleocapsid peptides P13 and P15, followed by 72% for the P10, and 67% for the P12 peptides from the spike protein (Figure 2B). Furthermore, all peptides had a specificity of 100%. The high specificity for these peptides was based on the high threshold used to determine positive and negative samples. We observed that some patients' samples had a higher OD signal with the nucleocapsid protein-based peptides, while others had a higher signal with the spike protein-based peptides. These results suggest that pooling or combining at least two peptides from the P10, P12, P13, and P15 could improve the sensitivity for detecting SARS-CoV-2 antibodies.

Screening All Samples

Peptides with the highest sensitivity and specificity, P10, P12, P13, and P15, were selected to be tested with all 110 positive and 35 negative samples. In addition, two FEPs combining the sequences of the P10 and P15 and one FEP combining the

https://doi.org/10.1021/acsbiomedchemau.3c00010
ACS Bio Med Chem Au 2024, 4, 37−52

sequences of the P12 and P13 peptides were synthesized as one long peptide. In this experiment, all samples were tested with single epitope (P10, P12, P13, and P15), mixed epitopes (P10 + P15 and P12 + P13), and fused-epitope (FEP10-15, FEP15-10, and FEP12-13) peptides. The fused-epitope peptides were designed to have one epitope from the spike protein and another epitope from the nucleocapsid protein. Moreover, the two FEPs from the P10 and P15 peptides were designed with flipped sequence to assess the role of peptide orientation on the test parameters. All peptides had a statistically significant difference in fluorescence signal intensity between the positive and negative samples (p-value < 0.0001) (Figure 3A–D). Moreover, the FEPs had a higher mean OD signal when compared with the single and mixed peptides but less than the spike protein control. Statistical comparison between the different peptides and spike protein is provided in Figure S13.

Receiver operating characteristics (ROC) curves were generated for all peptides, and the area under the curve (AUC) was calculated for each curve. Each peptide's sensitivity, specificity, and accuracy were determined using the optimal Youden's index from ROC curves; detailed information about the calculations is provided in the Experimental Section. The FEPs had higher AUCs compared to all single peptides (Figure 3E,F). Consistent with the AUC findings, FEP15-10 and FEP12-13 had the highest sensitivity, specificity, and accuracy in comparison to the single and mixed peptides; the FEP15-10 peptide had results similar to the spike protein control (Table 2). On the other hand, FEP10-15 had higher sensitivity, specificity, and accuracy than the single peptides but similar results to the mixed peptides. Since the P15 peptide had the maximum possible specificity, there was no increase in the specificity for FEP10-15 and FEP15-10. However, an improvement in all test parameters was observed for FEP12-13 because none of the single peptides reached the maximum sensitivity, specificity, or accuracy.

Additional experiments with the FEPs were performed. Two FEPs, FEP 15–10 and FEP12-13, were mixed to assess how pooling them would affect their sensitivity, specificity, and accuracy. The OD signal was higher for the mixed FEPs compared to the single FEPs for the positive samples (Figure 4). There was a significant improvement in the specificity for the mixed FEPs compared to the single FEP12-13 peptide; however, both sensitivity and specificity were lower for the mixed FEPs compared to the single FEP15-10 peptide, as shown in Table 2. This result indicates that the effect of mixing two antigens is not additive on the sensitivity, specificity, and accuracy outcomes. In the future, peptides with the highest possible specificity should be considered when testing the pooling of multiple peptides.

A previous study has used bioinformatics tools and reported that there is a potential to improve the sensitivity and specificity of SARS-CoV-2 antibody detection using a mixture of peptides.[14] The sensitivity could reach 100% when using a mixture of four peptides.[14] This enhancement in sensitivity and specificity has also been reported for a chemiluminescent immunoassay that uses multiple antigens for detecting SARS-CoV-2 antibodies.[25] These results are consistent with our own findings in this study, in which we experimentally demonstrated that both sensitivity and specificity increase when using a mixture of multiple peptides. We have also found that FEP combining sequences from different viral protein regions can further improve the sensitivity and specificity. Combining

Table 2. Sensitivity, Specificity, and Accuracy for P10, P12, P13, P15, Mixed P10 + P15, Mixed P12 + P13, FEP10-15, FEP15-10, and FEP12-13 Peptides

	P10	P12	P13	P15	P10 + P15	P12 + P13	FEP10-15	FEP15-10	FEP12-13	FEP15-10+ FEP12-13	spike protein
sensitivity (95% CI)	76.3% (64.5–84.5%)	66.3% (42.7–83.6%)	75.4% (46.3–83.6%)	70.9% (60.0–80.0%)	80% (70.0–88.1%)	80.0% (68.2–87.3%)	73.6% (67.3–85.4%)	88.2% (80.9–96.3%)	82.7% (77.3–91.8%)	82.7% (75.4–89.1%)	90.9% (85.4–95.4%)
specificity (95% CI)	91.4% (82.9–100%)	80.0% (62.9–100%)	68.6% (60.0–94.3%)	100% (91.4–100%)	100% (91.4–100%)	85.7% (77.1–97.1%)	100% (94.3–100%)	100% (91.4–100%)	88.6% (77.1–97.1%)	97.1% (91.4–100%)	100% (100%)
accuracy (95% CI)	79.3% (71.7–86.2%)	69.7% (55.9–78.6%)	73.8% (56.6–80.7%)	77.2% (69.7–84.1)	84.1% (77.2–90.3%)	81.4% (73.1–87.6%)	80% (75.2–87.6%)	90.3% (85.5–95.9%)	84.1% (79.3–91.0%)	86.2% (80.0–91.7%)	93.1% (89.0–96.6%)

https://doi.org/10.1021/acsbiomedchemau.3c00010
ACS Bio Med Chem Au 2024, 4, 37–52

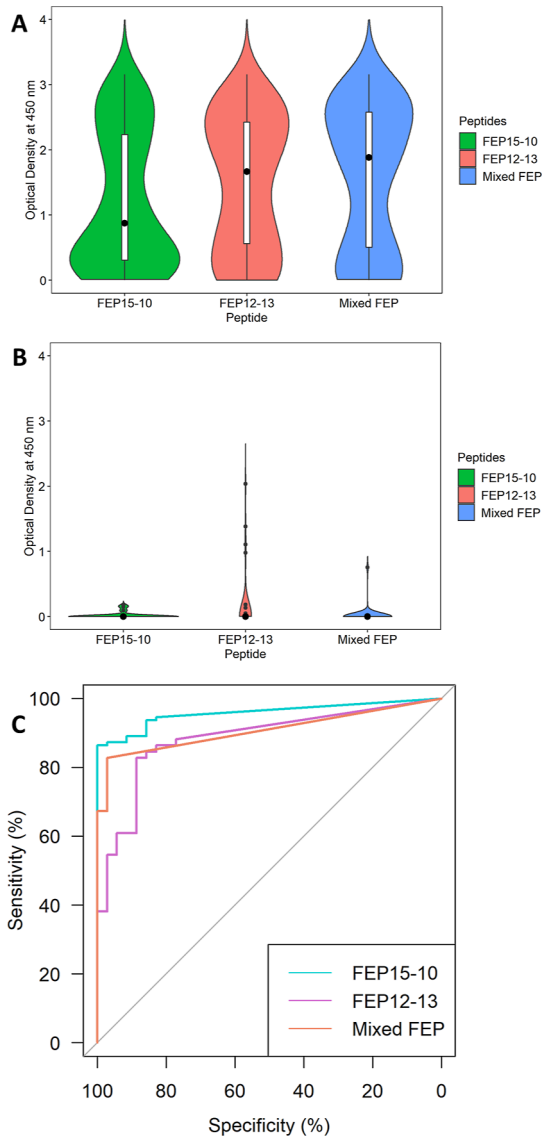

Figure 4. OD results for FEP 15−10, FEP 12−13, and mixed fusion epitope peptides when tested with (A) 110 IgG-positive COVID-19 samples and (B) 35 negative pre-COVID-19 samples. (C) ROC curves for the tested peptides.

different sequences has been demonstrated previously in which cell-penetrating peptides were combined with peptides that have DNA-binding activities in order to design multifunctional peptides.[26] However, FEPs are different from fusion peptides, which are epitopes on viral surface proteins that are responsible for viral entry into the host cell.[27,28] Our concept of the FEP is that two non-consecutive epitopes from the same protein or epitopes from two or more proteins are fused to create one peptide that can be used for antibody detection. Furthermore, FEPs could include epitopes from two different pathogens and are not limited to the same pathogen.

The better performance of the results for the FEPs over the single and mixed epitopes may be related to multiple factors. First, the enhancement may be due to the bigger molecular size of the FEPs that enhance the stability of secondary structures. This was observed in the predicted secondary structure of the two flipped FEPs in the computational studies: the longer sequence of FEPs can lead to a more stable tertiary structure. In addition, FEPs would have better exposure and accessibility to the antibodies by being more elevated above the assay plate. This was observed when the sequence of the fusion epitope was flipped: FEP15-10 had better results than FEP10-15. This may be due to the elevation of P10, which had slightly better test outcomes compared with P15 when they were tested as single peptides.

SARS-CoV-2 is an RNA virus that is susceptible to mutations. Several mutations have emerged since the beginning of the pandemic, five of which have been identified as variants of concern by the World Health Organization (WHO): Alpha, Beta, Gamma, Delta, and Omicron (Table S1).[29] Some of the mutations in these variants have resulted in changes to the amino acid sequences used in this study. For example, the Alpha variant has resulted in a change to the spike protein that affected our P10 peptide (A570D), while the Delta variant has resulted in a change to the nucleocapsid protein that affected our P15 peptide (D377Y).[30] However, none of the recent Omicron variants have caused any changes to the best-performing peptides in this study, which include P10, P12, P13, and P15. The extent to which these changes may affect the sensitivity and specificity of these peptides is yet to be determined. However, one of the advantages of our concept to use a FEP concept is that multiple sequences from different variants can be fused to detect antibodies from any variant.

In Silico Molecular Docking Simulations

To further elucidate the peptide-antibody interactions, an in silico analysis based on protein molecular docking was performed. The aim of this experiment was to simulate the docking between the peptides and antibodies. A general overview of the molecular docking simulations is presented in a graphical flowchart (Figure 5A). Initially, the peptides' three-dimensional structures were predicted using AlphaFold 2, a program developed for protein structure predictions (Figure 1, Figures S14−S23, Table S2).[31,32] The domains for most of the peptides seem to be in their majority random coils, and it was observed that some of the spike-derived peptides contain regions that fold into alpha-helical secondary structures (Figure 1). The presence of helical secondary structures was observed in peptides P5, P4, P10, P11, P12, and P14, which were selected from the RBD, S1, and S2 regions from the SARS-CoV-2 spike protein (Figure 1).

Circular Dichroism

The peptides' secondary structure was assessed using circular dichroism (CD). In line with the in silico simulation experiments, CD spectra showed alpha helical components for P5, P11, P12, P14, and FEP12-13 in which there is a positive band at 190 nm. On the other hand, P6, P7, P13, P15, FEP10-15, and FEP15-10 showed random coil structure in which there is a negative band at 190 nm. The CD spectra for all peptides are shown in Figure S24.

For each of the peptides, a protein data bank (PDB) database search was performed to identify which crystal structures of the SARS-CoV-2 antibodies bind to the corresponding regions of the spike and nucleocapsid proteins (Table S3). Selected antibody structures were then used for the peptide-antibody docking studies. Our selection criterion was to consider the highest degree of overlapping sequences between the antibodies and the individual peptide epitopes (Table S4). Except for the P15 peptide, we identified various antibodies that target the investigated peptides. An extensive number of reported antibodies bind to the RBD region of the

https://doi.org/10.1021/acsbiomedchemau.3c00010
ACS Bio Med Chem Au 2024, 4, 37−52

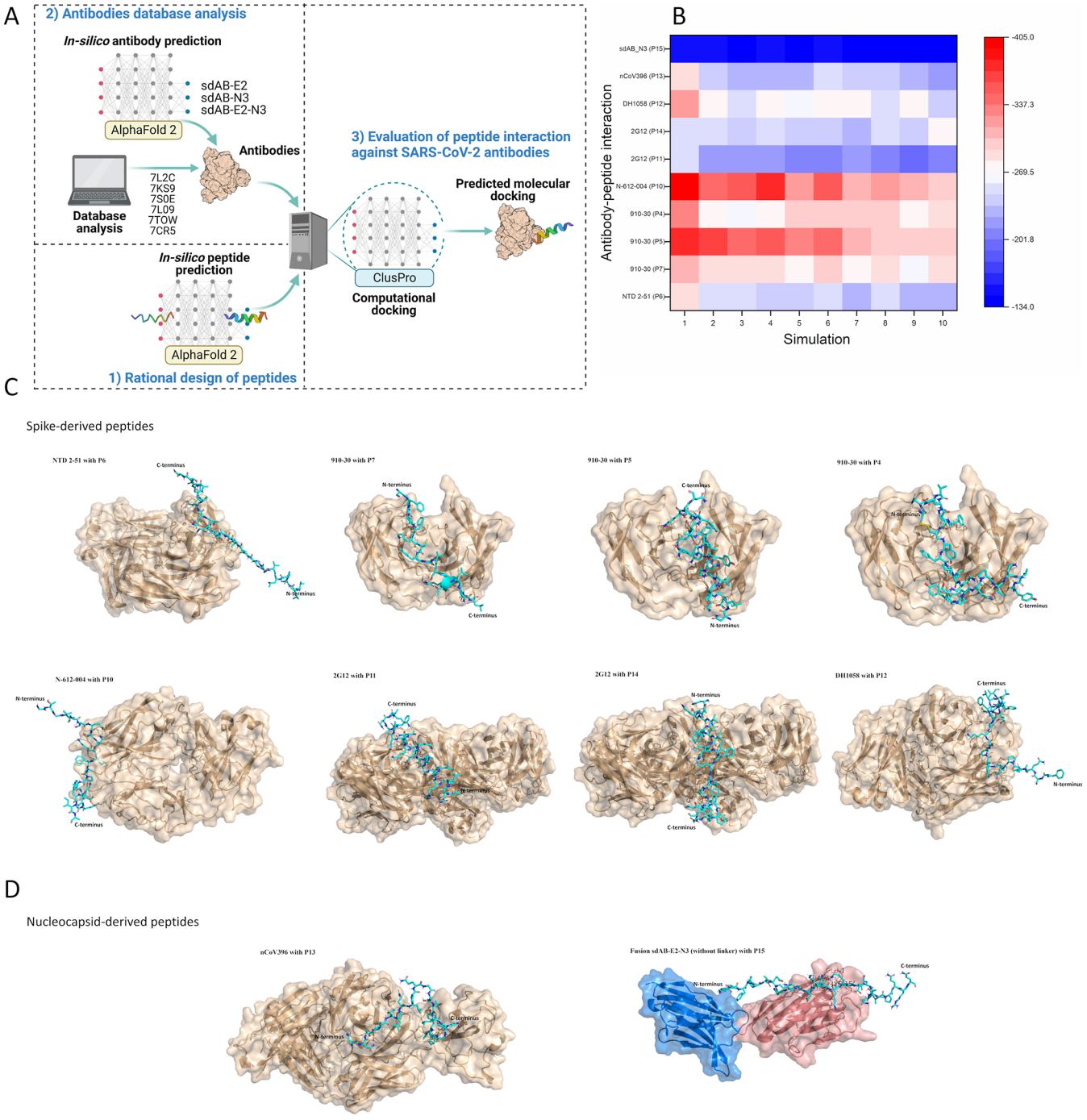

Figure 5. Graphical flowchart for the docking simulations (A). The top 10 simulations are identified according to their lowest energy scores (B). Docking interactions between the spike-derived peptides (C) and the nucleocapsid-derived peptides (D) against different SARS-CoV-2 antibodies. Antibodies used include NTD 2−51 (PBD: 7L2C), 910−930 (PBD: 7KS9), N-612-004 (PDB: 7S0E), 2G12 (PBD: 7L09), DH1058 (PDB: 7TOW), nCoV396 (PDB: 7CR5), and sdAB E2-N3.

SARS-CoV-2. By contrast, only limited number of antibodies are currently available that binds to regions outside of the RBD and to the nucleocapsid protein. The vast number of reported RBD-binding antibodies can be explained by the extensive number of neutralizing antibodies that target this region. Hence, most studies have focused on RBD-binding antibodies.[33−35] On the other hand, antibodies to the nucleocapsid protein of the SARS-CoV-2 have been reported to have better sensitivity than the spike protein antibodies, which make them suitable candidates for diagnostic assays.[36,37]

Since there is no reported PDB antibody structure that targets the P15 peptide epitope within the nucleocapsid protein, we utilized AlphaFold 2 to generate a prediction for an antibody structure targeting the N-CTD region of the nucleocapsid protein (Figure 1). This antibody was predicted using sequences reported by Ye et al.[38] Their study highlights the role of single-domain antibodies (sdABs) to target the N-CTD region. The authors report the protein sequences of two sdABs (sdAB-E2 and sdAB-N3) that interact with the N-CTD regions 247−364 and 365−419, respectively.[38] After an Alpha

https://doi.org/10.1021/acsbiomedchemau.3c00010
ACS Bio Med Chem Au 2024, 4, 37−52

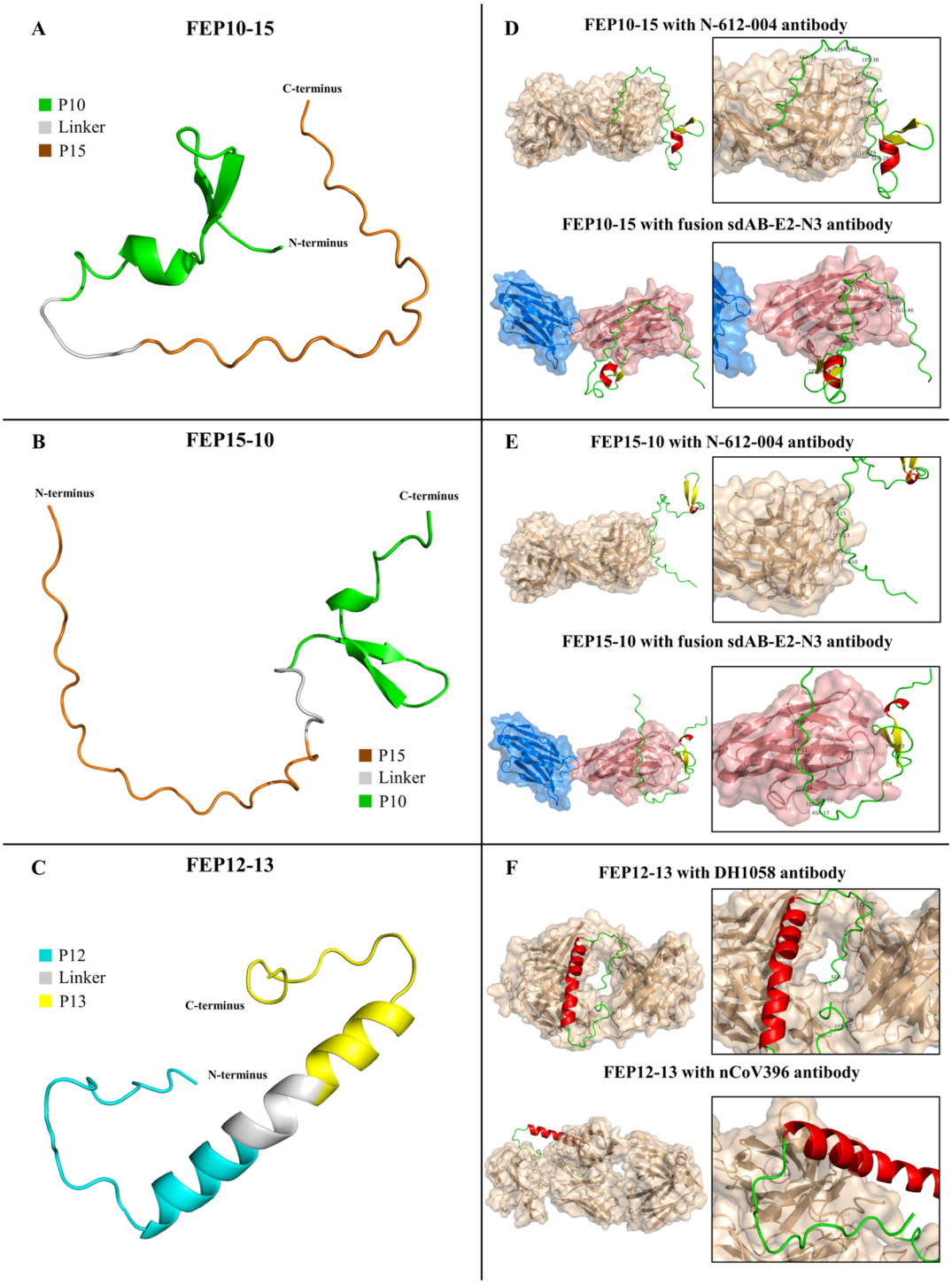

Figure 6. AlphaFold 2 three-dimensional structure prediction for (A) FEP10-15 (B) FEP15-10, and (C) FEP12-13 peptides. The molecular docking from (D) FEP10-15, (E) FEP15-10, and (F) FEP12-13. Antibodies used include N-612-004 (PDB: 7S0E), DH1058 (PDB: 7TOW), and nCoV396 (PDB: 7CR5). The FEP secondary structures were labeled in red (helix), yellow (sheet), and green (random coil), respectively (D–F).

Fold 2 modeling validation (see Experimental Section), a P15-recognizing antibody was predicted by combining the protein sequences of sdAB-E2 (nucleocapsid interacting region 247–364) and sdAB-N3 (nucleocapsid interacting region 365–419) to generate a fused antibody structure (sdAB-E2-N3; Table S5). We were satisfied that our reconstructed antibody model showed an accuracy of over 90% (Figure S25). The simulated, fused sdAB-E2-N3 antibody can be used for the interaction with the P15 peptide; however, further assessment will be needed when the crystal structures of more antibodies for the N-CTD region become available.

We used ClusPro, which is a tool used for protein-to-protein docking simulations, to assess the binding between the selected peptides and SARS-CoV-2 antibodies. The top 10 molecular docking simulations for the binding between the peptides and the corresponding SARS-CoV-2 antibodies were identified (Figure 5B), and the docking interactions are illustrated in Figure 5C. The results indicate that all the selected peptides

https://doi.org/10.1021/acsbiomedchemau.3c00010
ACS Bio Med Chem Au 2024, 4, 37–52

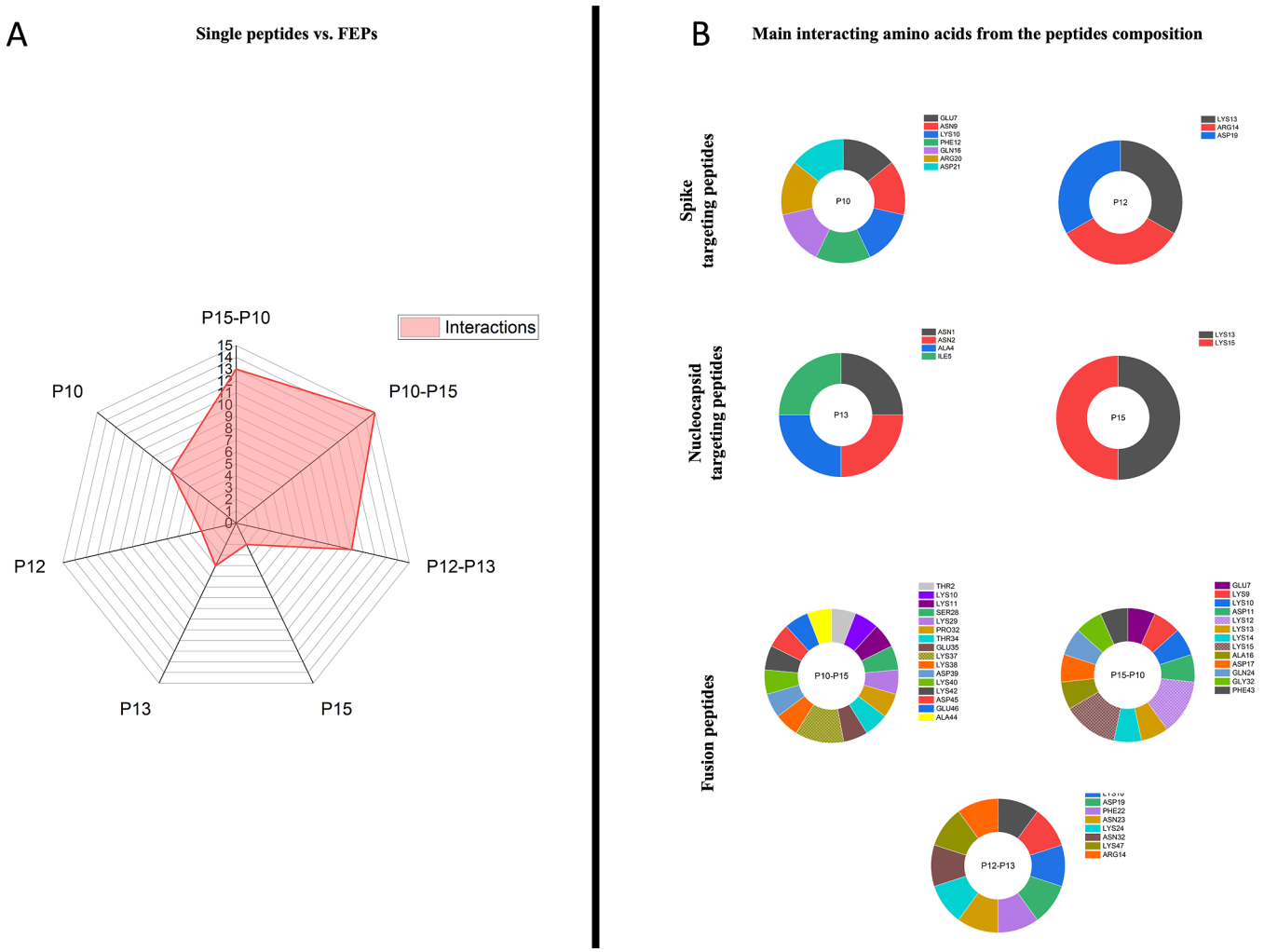

Figure 7. Comparison between single and FEPs' binding interactions against the SARS-CoV-2 antibodies (A). The main interacting amino acids from the peptide composition against the antibodies are shown; patterned colors represent the overlapping amino acids between the two antibodies (B).

from the spike and nucleocapsid regions interact with SARS-CoV-2 antibodies according to their modeled structure.

Next, we envisioned designing of FEPs to further enhance the binding with SARS-CoV-2 antibodies. In this case, the best-performing peptides from the spike and nucleocapsid proteins were selected, and their three-dimensional structures were predicted using AlphaFold 2, to carry out molecular docking simulations. These FEPs include FEP10-15, FEP15-10, and FEP12-13. It was found that both FEP15-10 and FEP10-15 folded similarly, exhibiting closely mirrored structures in which they shared the presence of alpha-helical and beta-sheet secondary structures (Figure 6A,B). On the other hand, the FEP12-13 mainly exhibited a helical structure (Figure 6C). More information about the accuracy of the AlphaFold 2 modeling to generate FEP structures is reported in Figures S26 and S27. The simulation between the FEPs and SARS-CoV-2 antibodies was performed using ClusPro and the structures are demonstrated in Figure 6D−F.

Our molecular binding results show that the FEPs exhibited higher interactions against SARS-CoV-2 antibodies in comparison to the single peptides. For the single peptide simulations, P10 was found to have the highest number of interactions, followed by P13, P12, and P15 (Figure 7A). On the other hand, FEP10-15 exhibited the most interactions against the tested antibodies, followed by FEP15-10 and FEP12-13; preliminary testing with FEP13-12 showed similar trends to the other FEPs (Figure 7 and Table S6). The evaluated FEPs had more interactions with the antibodies compared with the single peptides (Figure 7).

Since the FEPs can interact with antibodies from two different regions, a simulation was performed for each antibody and the interactions from the two simulations were combined to obtain the total number of interactions. FEP10-15 had a total of 13 unique amino acid interactions and two common interactions between the two antibodies, while FEP15-10 had 16 unique amino acid interactions and one common interaction between the two antibodies (Figure 7B). Unfortunately, the FEP simulation was restricted to testing each antibody individually and not as a pool of antibodies due to the limitations of the simulation tool. Future studies using more advanced simulations will be needed to study the docking between a pool of antibodies and the FEPs. Detailed information about the molecular docking studies is presented as part of the Supporting Information (Table S3).

The simulation data demonstrates the possibility of using AlphaFold 2 to predict the structure of antibodies to be used for the docking studies. Most of the studies in the literature report sequences of antibodies that can be used either to detect

https://doi.org/10.1021/acsbiomedchemau.3c00010
ACS Bio Med Chem Au 2024, 4, 37−52

or neutralize an antigen, but only a few, select studies report the macromolecular structures of these antibodies in the PDB database. These antibody sequences can be used with AlphFold 2 to predict the antibody's macromolecular structure for comprehensive computational studies. Furthermore, AlphaFold 2 could be utilized to generate more antibodies and predict all possible interacting amino acids from each peptide in the future. With more advanced simulations, the sequences of FEPs could be optimized to design peptides that are more stable, enhance interactions, and omit overlaps, resulting in enhanced sensitivity and specificity.

Future Directions

The antigens used in this study, either as individual peptides or FEPs, could be used to develop serological tests for commercial applications. For example, an ELISA test similar to the one used in this study could be developed and made commercially available as a coated plate to detect serum antibodies in all clinical laboratories. Another possible application involves conjugating magnetic beads with these peptide epitopes to detect serum antibodies using a magnetic chemiluminescence immunoassay, as used in more advanced clinical laboratories.[39] In these assays, there is still a need to find an optimal antigen for better antibody detection, as recently highlighted by Rosadas et al.[40] Furthermore, these peptide epitopes could be used to develop rapid serological tests to detect SARS-CoV-2 antibodies. For example, a lateral flow immunoassay (LFIA) could be developed for the rapid detection of SARS-CoV-2 antibodies.[41,42] In addition, conjugating peptide epitopes to gold nanoparticles could enable rapid detection of antibodies using a nanosensor colorimetric assay.[43] These rapid tests could be used as point-of-care tests where access to a clinical laboratory is limited.

CONCLUSIONS

In this study, we have demonstrated that the sensitivity, specificity, and accuracy of a peptide-based immunoassay can be improved by using a FEP. Two epitopes from the SARS-CoV-2 spike protein and two epitopes from the nucleocapsid protein were selected and FEPs were synthesized by combining the sequences from one spike and one nucleocapsid epitopes. A docking simulation demonstrated the binding between these FEPs and SARS-SoV-2 antibodies and highlighted the interacting amino acids from the FEP peptides. Multiplex testing with FEPs showed better sensitivity, specificity, and accuracy compared with multiplex testing with a mixture of single epitope peptide antigens. Moreover, synthesis of a FEP has the advantage of being both time- and cost-efficient by synthesizing one peptide as opposed to the double effort required for two peptides. Thus, peptide epitopes could be used to design immunoassays to detect SARS-SoV-2 antibodies, either as a point-of-care or laboratory-based test, with higher sensitivity and specificity. Moreover, due to the flexibility of peptide synthesis, peptide epitope sequences could be quickly modified and synthesized to reflect changes in the SARS-CoV-2 sequence due to mutations. Future simulation and experimental studies could be conducted to tailor-make FEPs with improved sensitivity, specificity, and accuracy. We hope that this encouraging concept can be applied to improve the lateral flow immunoassay test to a level that is comparable to a laboratory-based test. Finally, this concept is not limited to SARS-CoV2, but can be applied to any other diseases that require immunoassays with a high degree of sensitivity and specificity.

EXPERIMENTAL SECTION

Peptide Selection and Peptide Synthesis

Peptide Design. B-cell epitopes were selected from the SARS-CoV-2 proteins based on emerging computational and experimental epitope-mapping studies.[12−14,22,23] A biotin tag was incorporated into the peptide epitopes at the N-terminal site. Figure 1 maps the synthesized peptide sequences to the spike and nucleocapsid proteins. A "SGSGS" linker was used between the epitopes in the FEPs, because its flexibility permits the mobility of the linked parts without it interfering with the function of each domain.[44] The entire sequences are provided in Table 1.

Peptide Synthesis and Purification. All peptide epitopes were synthesized via solid-phase peptide synthesis (SPPS) using a CS136X CS Biopeptide synthesizer. The peptide coupling was conducted on MBHA Rink amide resin, agitated in a mixture of TBTU (3 equiv), HOBt (3 equiv), DIPEA (6 equiv), and Fmoc-protected amino acid (3 equiv) for an hour. The resin was then washed with DMF (3×), DCM (3×), and DMF (3×). A 20% (v/v) piperidine/DMF solution was subsequently added to remove the Fmoc-protecting group from the sequence. These steps of coupling, washing, and Fmoc deprotection were repeated until the desired sequence was achieved. In every sequence, the last amino acid coupled was Fmoc-Lys(Biotin)−OH. The resin was then transferred out of the synthesizer and cleaved with an acidic solution of TFA/TIS/water (95:2.5:2.5). After 2 h of mixing, the solution was collected, dispersed in cold diethyl ether, and stored at 4 °C overnight. The precipitated peptide was then centrifuged and dried in a vacuum desiccator prior to being purified. Peptide purification was performed with reversed-phase high-performance liquid chromatography using the C-18 column.

Liquid Chromatography-Mass Spectroscopy. The peptide purity was determined using a Dionex ultra high-pressure liquid chromatography system (nano RSLC) equipped with either Orbitrap Lumos Tribrid mass spectrometer (Thermo Scientific) or Orbitrap Exploris 480 mass spectrometer (Thermo Scientific). Peptides (125 ng) were injected onto a 75 μm × 2 cm PepMap-C18 pre-column and resolved on a 3 μm, 100 Å particle size 75 μm × 15 cm RP-C18 EASY-Spray temperature controlled integrated column-emitter (Thermo), using a 30 min multistep gradient from 2.1% B to 55% B with a constant flow of 300 nL min^{-1}. After that, percentage B was increased to 95% and maintained for 5 min to ensure all peptides are eluted before finally equilibrating the column from t = 36 to t = 45 min at 2.1% B. The mobile phases were: Water incorporating 0.1% FA (solvent A) and 95% ACN incorporating 0.1% FA (solvent B). The spray was initiated by applying 2 kV to the EASY-Spray emitter and the data were acquired under the control of Xcalibur software (Version 4.3, June 2019) in a data-dependent mode using top speed and 2 s duration per cycle. The scan survey was acquired in the Orbitrap in the high mass mode covering the m/z range from 500 to 3500 Th for Orbitrap Lumos and 350 to 1400 Th for Orbitrap Lumos. The results were then analyzed using Thermo Scientific FreeStyle software (version 1.8 SP1). Spectra for the tested peptides are provided in Figures S1−S12.

Patient Samples

The serum samples of patients were obtained from King Khalid Teaching Hospital and King Fahad Medical City in Riyadh, Saudi Arabia. This study was approved by the institutional review board committee (IRB) at both institutions and the institutional ethics and biosafety committee (IBEC) at King Abdullah University of Science and Technology (KAUST). A total of 145 samples were used, comprising 110 samples collected from PCR-confirmed COVID-19 patients and 35 pre-COVID-19 samples collected and archived before outbreak, which were used as a negative control. All samples collected from COVID-19 patients tested positive for the presence of SARS-SoV-2 antibodies using a commercial antibody test (Abbott COVID

https://doi.org/10.1021/acsbiomedchemau.3c00010
ACS Bio Med Chem Au 2024, 4, 37−52

IgG) at King Khalid Teaching Hospital's clinical laboratory. In addition, the age, gender, date of PCR testing, and date of blood sample collection were recorded for each sample.

ELISA Experiment: All Antigens Screening

ELISA was performed using streptavidin-coated plates (Thermo Fisher, Cat# 15120). A detailed outline of the ELISA protocol is provided in the Supporting Information. Initially, experiments were conducted with a single peptide coating at a concentration of 1 μM and S1 spike protein (SinoBiological, 40591-V08H) at a concentration of 2 μg/mL, in which 18 positive and six negative samples, all randomly selected, were tested. The peptides tested included P4, P5, P6, P7, P10, P11, P12, P13, P14, and P15 (Figure 1, Table 1). In addition, control wells with no peptide coating were used to correct for background signal.[45] Next, peptides with the highest sensitivity and specificity were selected and tested with more patients' samples, as outlined below.

ELISA Experiment: All Samples Screening

Two peptides from the spike protein (P10 and P12) and two from the nucleocapsid protein (P13 and P15) were selected to be tested with all 110 positive samples and 35 negative pre-COVID-19 samples. Additionally, the sequences from the P10, P15, P12, and P13 peptides were combined and synthesized as three longer FEPs (FEP10-15, FEP15-10, and FEP12-13). The FEPs and a mixture of the corresponding single peptides were tested with all samples. The data from the single peptides, the single peptides mixture, the FEPs, and the spike protein control were compared to assess any change in the sensitivity, specificity, and accuracy. Furthermore, additional experiments were conducted with a mixture of FEP15-10 and FEP12-13 to any evaluate changes in sensitivity, specificity, and accuracy.

ELISA Data Analysis

Optical density (OD) data correction was performed for all tested samples. The mean optical density (OD) signal from wells coated with a peptide was calculated and subtracted from the mean OD signal for the peptide control wells, which were wells with no peptide coating. The corrected data from the negative pre-COVID-19 samples were used to calculate the threshold value for each peptide.

All Antigens Screening Analysis. For the peptide screening experiment, the threshold used to determine positive and negative results was determined using the following formula: mean of OD signal of negative samples + (3 × SD).[46] Any sample with an OD result above the threshold would be considered positive, and any sample with an OD result below the threshold would be considered negative. Furthermore, sensitivity, specificity, and accuracy were calculated for each peptide using the following formulas:

$$\text{sensitivity} = \frac{\text{true positive}}{\text{true positive} + \text{false negative}} \times 100\% \quad (1)$$

$$\text{specifity} = \frac{\text{true negative}}{\text{true negative} + \text{false positive}} \times 100\% \quad (2)$$

$$\text{accuracy} = \frac{\text{true positive} + \text{true negative}}{\text{all samples}} \times 100\% \quad (3)$$

All Samples Screening Analysis. OD results for all samples tested with the single peptides, mixed peptides, and FEPs were compared using the Mann–Whitney *U* test (Wilcoxon Rank Sum Test). Furthermore, ROC curves were computed and analyzed to assess the AUC for each peptide.[47] Besides this, the optimal threshold was determined using Youden's J statistics[48] to determine the sensitivity, specificity, and accuracy for each peptide; a 95% confidence interval was calculated with 2000 bootstrap. Statistical analysis was performed using R 4.1.0 software.

Docking Simulations

The molecular docking between the peptides and antibodies was simulated to further elucidate the binding of the peptides to the spike and nucleocapsid antibodies. Several peptides based on the SARS-CoV-2 spike protein (P4, P5, P6, P7, P10, P11, P12, and P14) and two peptides from the nucleocapsid protein (P13 and P15) were used as targets for the reported antibodies. The PDB database was searched for antibodies that target the SARS-CoV-2 proteins that correspond to our peptide sequences (Table S3). The following antibodies were included: NTD 2–51 (PBD: 7L2C), 910–930 (PBD: 7KS9), N-612-004 (PDB: 7S0E), 2G12 (PBD: 7L09), DH1058 (PDB: 7TOW), and nCoV396 (PDB: 7CR5), which have been reported to interact with different regions from the spike and nucleocapsid protein (Table S3).[49−54] The protein sequences of the sdABs E2 and N3 were discovered in the literature.[38] The initial tridimensional configuration of the single peptides and FEPs was determined with AlphaFold 2 using MMseqs2.[31,32] In addition, the prediction of the structure of sdAB E2-N3 was determined with AlphaFold 2. A control was developed to test the accuracy of AlphaFold 2 by predicting the already-reported heavy chain of the antibody nCoV396 (PDB: 7CR5; Figure S28). Then, docking simulations between the resulting peptide configurations and the isolated antibodies were performed according to the ClusPro protein–protein antibody docking methodology.[55−59] A negative control was developed by docking antibodies for the nucleocapsid to the spike protein-derived peptides and vice versa. Next, the top 10 simulations of each docking were determined through their lowest energy scores. The interactions were visualized and analyzed using PyMOL (v4.6.0).

Circular Dichroism

CD spectra were measured at scanning wavelengths between 190 and 300 nm with 1.0 nm using an AVIV-430 spectrophotometer. All peptides were dissolved in 20% TFE at a concentration of 1 mg/mL in a 0.1 mm optical pathlength cuvette and the signals were normalized to the molar ellipticity value. P4 peptide was not dissolving properly so it was included in the analysis.

■ ASSOCIATED CONTENT

Supporting Information

The Supporting Information is available free of charge at https://pubs.acs.org/doi/10.1021/acsbiomedchemau.3c00010.

Peptide selection and peptide synthesis; ELISA protocol; SARS-CoV-2 variants of interest; selected models from the AlphaFold2 peptide's three-dimensional structure predictions; five top models were generated for each of the peptide structures; screening of SARS-CoV-2 antibodies for the docking simulation; molecular docking simulations peptides and antibodies; P15 region antibody protein sequence; peptides binding interactions; characterization of P5 using LC-MS; characterization of P6 using LC-MS; characterization of P7 using LC-MS; characterization of P10 using LC-MS; characterization of P11 using LC-MS; characterization of P12 using LC-MS; characterization of P13 using LC-MS; characterization of P14 using LC-MS; characterization of P15 using LC-MS; characterization of P10-P15 using LC-MS; characterization of P15-P10 using LC-MS; characterization of P12-P13 using LC-MS; statistical comparison between the different tested peptides and spike protein control; AlphaFold 2 three-dimensional structure prediction for P6 peptide; AlphaFold 2 three-dimensional structure prediction for P7 peptide; AlphaFold 2 three-dimensional structure prediction for P5 peptide; AlphaFold 2 three-dimensional structure prediction for P4 peptide; AlphaFold 2 three-dimensional structure prediction for P10 peptide; AlphaFold 2 three-dimensional structure prediction for P11 peptide; AlphaFold 2 three-dimensional structure prediction for P14 peptide; AlphaFold 2 three-dimensional structure prediction for P12 peptide; AlphaFold 2 three-dimen-

https://doi.org/10.1021/acsbiomedchemau.3c00010
ACS Bio Med Chem Au 2024, 4, 37−52

sional structure prediction for P13 peptide; AlphaFold 2 three-dimensional structure prediction for P15 peptide; circular dichroism (CD) spectra for the single and FEP peptides; AlphaFold 2 three-dimensional structure prediction for the fusion sdAB-E2-N3; AlphaFold 2 three-dimensional structure prediction for the fusion peptides FEP15-10 and FEP10-15; AlphaFold 2 three-dimensional structure prediction for the fusion peptide FEP12-13; and comparison of the AlphaFold 2 three-dimensional structure prediction for the heavy chain of the antibody 7CR5 against the reported X-ray diffraction structure (PDF)

AUTHOR INFORMATION

Corresponding Author

Charlotte A. E. Hauser − *Laboratory for Nanomedicine, Division of Biological and Environmental Science and Engineering (BESE), King Abdullah University of Science and Technology (KAUST), Thuwal 23955-6900, Saudi Arabia; Computational Bioscience Research Center (CBRC), King Abdullah University of Science and Technology, Thuwal 23955-69900, Saudi Arabia; Red Sea Research Center, Division of Biological and Environmental Science and Engineering (BESE), King Abdullah University of Science and Technology, Thuwal 23955-6900, Saudi Arabia;* orcid.org/0000-0001-8251-7246; Email: charlotte.hauser@kaust.edu.sa

Authors

Ali H. Aldoukhi − *Laboratory for Nanomedicine, Division of Biological and Environmental Science and Engineering (BESE), King Abdullah University of Science and Technology (KAUST), Thuwal 23955-6900, Saudi Arabia; Computational Bioscience Research Center (CBRC), King Abdullah University of Science and Technology, Thuwal 23955-69900, Saudi Arabia;* orcid.org/0000-0001-7949-4637

Panayiotis Bilalis − *Laboratory for Nanomedicine, Division of Biological and Environmental Science and Engineering (BESE), King Abdullah University of Science and Technology (KAUST), Thuwal 23955-6900, Saudi Arabia; Computational Bioscience Research Center (CBRC), King Abdullah University of Science and Technology, Thuwal 23955-69900, Saudi Arabia;* orcid.org/0000-0002-5809-9643

Dana M. Alhattab − *Laboratory for Nanomedicine, Division of Biological and Environmental Science and Engineering (BESE), King Abdullah University of Science and Technology (KAUST), Thuwal 23955-6900, Saudi Arabia; Computational Bioscience Research Center (CBRC), King Abdullah University of Science and Technology, Thuwal 23955-69900, Saudi Arabia;* orcid.org/0000-0002-0509-6182

Alexander U. Valle-Pérez − *Laboratory for Nanomedicine, Division of Biological and Environmental Science and Engineering (BESE), King Abdullah University of Science and Technology (KAUST), Thuwal 23955-6900, Saudi Arabia; Computational Bioscience Research Center (CBRC), King Abdullah University of Science and Technology, Thuwal 23955-69900, Saudi Arabia;* orcid.org/0000-0001-7317-4202

Hepi H. Susapto − *Laboratory for Nanomedicine, Division of Biological and Environmental Science and Engineering (BESE), King Abdullah University of Science and Technology (KAUST), Thuwal 23955-6900, Saudi Arabia; Computational Bioscience Research Center (CBRC), King Abdullah University of Science and Technology, Thuwal 23955-69900, Saudi Arabia;* orcid.org/0000-0003-3161-995X

Rosario Pérez-Pedroza − *Laboratory for Nanomedicine, Division of Biological and Environmental Science and Engineering (BESE), King Abdullah University of Science and Technology (KAUST), Thuwal 23955-6900, Saudi Arabia; Computational Bioscience Research Center (CBRC), King Abdullah University of Science and Technology, Thuwal 23955-69900, Saudi Arabia*

Emiliano Backhoff-García − *Laboratory for Nanomedicine, Division of Biological and Environmental Science and Engineering (BESE), King Abdullah University of Science and Technology (KAUST), Thuwal 23955-6900, Saudi Arabia*

Sarah M. Alsawaf − *Laboratory for Nanomedicine, Division of Biological and Environmental Science and Engineering (BESE), King Abdullah University of Science and Technology (KAUST), Thuwal 23955-6900, Saudi Arabia; Computational Bioscience Research Center (CBRC), King Abdullah University of Science and Technology, Thuwal 23955-69900, Saudi Arabia*

Salwa Alshehri − *Laboratory for Nanomedicine, Division of Biological and Environmental Science and Engineering (BESE), King Abdullah University of Science and Technology (KAUST), Thuwal 23955-6900, Saudi Arabia; Computational Bioscience Research Center (CBRC), King Abdullah University of Science and Technology, Thuwal 23955-69900, Saudi Arabia;* Present Address: Department of Biochemistry, Faculty of Science, University of Jeddah, Jeddah 23218, Saudi Arabia

Hattan Boshah − *Laboratory for Nanomedicine, Division of Biological and Environmental Science and Engineering (BESE), King Abdullah University of Science and Technology (KAUST), Thuwal 23955-6900, Saudi Arabia; Computational Bioscience Research Center (CBRC), King Abdullah University of Science and Technology, Thuwal 23955-69900, Saudi Arabia*

Abdulelah A. Alrashoudi − *Laboratory for Nanomedicine, Division of Biological and Environmental Science and Engineering (BESE), King Abdullah University of Science and Technology (KAUST), Thuwal 23955-6900, Saudi Arabia; Computational Bioscience Research Center (CBRC), King Abdullah University of Science and Technology, Thuwal 23955-69900, Saudi Arabia*

Waleed A. Aljabr − *Research Centre, King Fahad Medical City, Riyadh 12231, Saudi Arabia*

Manal Alaamery − *Developmental Medicine Department, King Abdullah International Medical Research Center, King Abdulaziz Medical City, Ministry of National Guard-Health Affairs, King Saud Bin Abdulaziz University for Health Sciences, Riyadh 11426, Saudi Arabia; KACST-BWH Centre of Excellence for Biomedicine, Joint Centers of Excellence Program, King Abdulaziz City for Science and Technology (KACST), Riyadh 12371, Saudi Arabia; Saudi Human Genome Project (SHGP), Satellite Lab at King Abdulaziz Medical City (KAMC), Ministry of National Guard Health*

https://doi.org/10.1021/acsbiomedchemau.3c00010
ACS Bio Med Chem Au 2024, 4, 37−52

Affairs (MNG-HA), King Abdulaziz City for Science and Technology (KACST), Riyadh 11426, Saudi Arabia

May Alrashed − *Department of Clinical Laboratory Science, College of Applied Medical Sciences, King Saud University, Riyadh 11433, Saudi Arabia; Chair of Medical and Molecular Genetics Research, King Saud University, Riyadh 11433, Saudi Arabia*

Rana M. Hasanato − *Department of Pathology and Laboratory Medicine, King Saud University, Riyadh 11433, Saudi Arabia*

Raed A. Farzan − *Department of Clinical Laboratory Science, College of Applied Medical Sciences, King Saud University, Riyadh 11433, Saudi Arabia; Chair of Medical and Molecular Genetics Research, King Saud University, Riyadh 11433, Saudi Arabia*

Roua A. Alsubki − *Department of Clinical Laboratory Science, College of Applied Medical Sciences, King Saud University, Riyadh 11433, Saudi Arabia; Chair of Medical and Molecular Genetics Research, King Saud University, Riyadh 11433, Saudi Arabia*

Manola Moretti − *Laboratory for Nanomedicine, Division of Biological and Environmental Science and Engineering (BESE), King Abdullah University of Science and Technology (KAUST), Thuwal 23955-6900, Saudi Arabia; Computational Bioscience Research Center (CBRC), King Abdullah University of Science and Technology, Thuwal 23955-69900, Saudi Arabia;* orcid.org/0000-0003-0171-4921

Malak S. Abedalthagafi − *Pathology and Laboratory Medicine, Emory School of Medicine, Atlanta, Georgia 30329, United States*

Complete contact information is available at: https://pubs.acs.org/10.1021/acsbiomedchemau.3c00010

Author Contributions

A.H.A., P.B., D.A., A.U.V.P., contributed equally to this work. The peptides were synthesized and purified by P.B., H.H.S., and S.A. ELISA studies were performed by A.H.A. and D.A., and ELISA optimization was performed by A.H.A., D.A., S.A., and H.B. Experimental design and analysis was performed by A.H.A., P.B., D.A., and M.M. The three-dimensional structure prediction of the peptides and the de novo design of the single-domain antibodies was performed by A.U.V.P. Molecular docking simulations were performed by A.U.V.P., R.P.P., and E.G.B. The simulations results were processed and analyzed by A.U.V.P. Experimental support was provided by A.A., R.H., W.A., M.A., R.A., R.F., M.A., and M.A. C.A.E.H. developed the concept and supervised the project. All authors contributed to the manuscript and approved the final version of the manuscript. CRediT: **Ali H Aldoukhi** data curation (equal), formal analysis (equal), investigation (equal), validation (equal), writing-original draft (equal); **Charlotte A. E. Hauser** conceptualization (lead), formal analysis (equal), funding acquisition (lead), resources (lead), supervision (lead), writing-review & editing (equal).

Funding

This work was financially supported by King Abdullah University of Science and Technology (KAUST) and by King Abdulaziz City for Science and Technology (KACST) with a funded grant (4419-KACST COVID-19).

Notes

The authors declare no competing financial interest.

■ ACKNOWLEDGMENTS

This work was financially supported by King Abdullah University of Science and Technology (KAUST) and by King Abdulaziz City for Science and Technology (KACST) with a funded grant (4419-KACST COVID-19). The authors acknowledge Mauricio Andres Aguilar Aguila Isaias for his support in creating the graphical abstract.

■ ABBREVIATIONS

SARS-CoV-2	severe acute respiratory syndrome corona virus 2
COVID-19	coronavirus disease 2019
ACE	angiotensin-converting enzyme
PCR	polymerase chain reaction
ELISA	enzyme-linked immunosorbent assay
CLIA	chemiluminescence immunoassay
FEP	fusion-epitopes peptides
SPPS	solid-phase peptide synthesis
IRB	Institutional Review Board
IBEC	Institutional Ethics and Biosafety Committee (IBEC)
RBD	receptor binding domain
OD	optical density
ROC	receiver operating characteristics
AUC	area under the curve
LFIA	lateral flow immunoassay

■ REFERENCES

(1) Guan, W. J.; Ni, Z. Y.; Hu, Y.; Liang, W. H.; Ou, C. Q.; He, J. X.; Liu, L.; Shan, H.; Lei, C. L.; Hui, D. S. C.; Du, B.; Li, L. J.; Zeng, G.; Yuen, K. Y.; Chen, R. C.; Tang, C. L.; Wang, T.; Chen, P. Y.; Xiang, J.; Li, S. Y.; Wang, J. L.; Liang, Z. J.; Peng, Y. X.; Wei, L.; Liu, Y.; Hu, Y. H.; Peng, P.; Wang, J. M.; Liu, J. Y.; Chen, Z.; Li, G.; Zheng, Z. J.; Qiu, S. Q.; Luo, J.; Ye, C. J.; Zhu, S. Y.; Zhong, N. S. Clinical Characteristics of Coronavirus Disease 2019 in China. *N. Engl. J. Med.* **2020**, *382*, 1708−1720.

(2) Cui, J.; Li, F.; Shi, Z. L. Origin and Evolution of Pathogenic Coronaviruses. *Nat. Rev. Microbiol.* **2019**, *17*, 181−192.

(3) To, K. K.; Tsang, O. T.; Leung, W. S.; Tam, A. R.; Wu, T. C.; Lung, D. C.; Yip, C. C.; Cai, J. P.; Chan, J. M.; Chik, T. S.; Lau, D. P.; Choi, C. Y.; Chen, L. L.; Chan, W. M.; Chan, K. H.; Ip, J. D.; Ng, A. C.; Poon, R. W.; Luo, C. T.; Cheng, V. C.; Chan, J. F.; Hung, I. F.; Chen, Z.; Chen, H.; Yuen, K. Y. Temporal Profiles of Viral Load in Posterior Oropharyngeal Saliva Samples and Serum Antibody Responses During Infection by Sars-Cov-2: An Observational Cohort Study. *Lancet Infect. Dis.* **2020**, *20*, 565−574.

(4) Zou, L.; Ruan, F.; Huang, M.; Liang, L.; Huang, H.; Hong, Z.; Yu, J.; Kang, M.; Song, Y.; Xia, J.; Guo, Q.; Song, T.; He, J.; Yen, H. L.; Peiris, M.; Wu, J. Sars-Cov-2 Viral Load in Upper Respiratory Specimens of Infected Patients. *N. Engl. J. Med.* **2020**, *382*, 1177−1179.

(5) Venter, M.; Richter, K. Towards Effective Diagnostic Assays for Covid-19: A Review. *J. Clin. Pathol.* **2020**, *73*, 370−377.

(6) Pan, X.; Kaminga, A. C.; Chen, Y.; Liu, H.; Wen, S. W.; Fang, Y.; Jia, P.; Liu, A. Auxiliary Screening Covid-19 by Serology. *Front. Public Health* **2022**, *10*, 819841.

(7) Deeks, J. J.; Dinnes, J.; Takwoingi, Y.; Davenport, C.; Spijker, R.; Taylor-Phillips, S.; Adriano, A.; Beese, S.; Dretzke, J.; Ferrante di Ruffano, L.; Harris, I. M.; Price, M. J.; Dittrich, S.; Emperador, D.; Hooft, L.; Leeflang, M. M.; Van den Bruel, A.; Cochrane, C.-D. T. A. G. Antibody Tests for Identification of Current and Past Infection with Sars-Cov-2. *Cochrane Database Syst. Rev.* **2020**, *2020*, CD013652.

(8) Kohl, T. O.; Ascoli, C. A. Indirect Immunometric Elisa. *Cold Spring Harb. Protoc.* **2017**, *2017*, pdb.prot093708.
(9) Mishra, A. R.; Hutke, V. R.; Satav, A. R.; Ali, S. A.; Daginawala, H. F.; Singh, L. R.; Kashyap, R. S. Synthetic Peptides Are Better Than Native Antigens for Development of Elisa Assay for Diagnosis of Tuberculosis. *Int. J. Pept. Res. Ther.* **2017**, *23*, 247−257.
(10) Petherick, A. Developing Antibody Tests for Sars-Cov-2. *Lancet* **2020**, *395*, 1101−1102.
(11) Groß, A.; Hashimoto, C.; Sticht, H.; Eichler, J. Synthetic Peptides as Protein Mimics. *Front. Bioeng. Biotechnol.* **2015**, *3*, 211.
(12) Poh, C. M.; Carissimo, G.; Wang, B.; Amrun, S. N.; Lee, C. Y.; Chee, R. S.; Fong, S. W.; Yeo, N. K.; Lee, W. H.; Torres-Ruesta, A.; Leo, Y. S.; Chen, M. I.; Tan, S. Y.; Chai, L. Y. A.; Kalimuddin, S.; Kheng, S. S. G.; Thien, S. Y.; Young, B. E.; Lye, D. C.; Hanson, B. J.; Wang, C. I.; Renia, L.; Ng, L. F. P. Two Linear Epitopes on the Sars-Cov-2 Spike Protein That Elicit Neutralising Antibodies in Covid-19 Patients. *Nat. Commun.* **2020**, *11*, 2806.
(13) Alves, D.; Curvello, R.; Henderson, E.; Kesarwani, V.; Walker, J. A.; Leguizamon, S. C.; McLiesh, H.; Raghuwanshi, V. S.; Samadian, H.; Wood, E. M.; McQuilten, Z. K.; Graham, M.; Wieringa, M.; Korman, T. M.; Scott, T. F.; Banaszak Holl, M. M.; Garnier, G.; Corrie, S. R. Rapid Gel Card Agglutination Assays for Serological Analysis Following Sars-Cov-2 Infection in Humans. *ACS Sens.* **2020**, *5*, 2596−2603.
(14) Amrun, S. N.; Lee, C. Y.; Lee, B.; Fong, S. W.; Young, B. E.; Chee, R. S.; Yeo, N. K.; Torres-Ruesta, A.; Carissimo, G.; Poh, C. M.; Chang, Z. W.; Tay, M. Z.; Chan, Y. H.; Chen, M. I.; Low, J. G.; Tambyah, P. A.; Kalimuddin, S.; Pada, S.; Tan, S. Y.; Sun, L. J.; Leo, Y. S.; Lye, D. C.; Renia, L.; Ng, L. F. P. Linear B-Cell Epitopes in the Spike and Nucleocapsid Proteins as Markers of Sars-Cov-2 Exposure and Disease Severity. *EBioMedicine* **2020**, *58*, 102911.
(15) Farrera-Soler, L.; Daguer, J. P.; Barluenga, S.; Vadas, O.; Cohen, P.; Pagano, S.; Yerly, S.; Kaiser, L.; Vuilleumier, N.; Winssinger, N. Identification of Immunodominant Linear Epitopes from Sars-Cov-2 Patient Plasma. *PLoS One* **2020**, *15*, No. e0238089.
(16) Li, Y.; Lai, D. Y.; Lei, Q.; Xu, Z. W.; Wang, F.; Hou, H.; Chen, L.; Wu, J.; Ren, Y.; Ma, M. L.; Zhang, B.; Chen, H.; Yu, C.; Xue, J. B.; Zheng, Y. X.; Wang, X. N.; Jiang, H. W.; Zhang, H. N.; Qi, H.; Guo, S. J.; Zhang, Y.; Lin, X.; Yao, Z.; Pang, P.; Shi, D.; Wang, W.; Yang, X.; Zhou, J.; Sheng, H.; Sun, Z.; Shan, H.; Fan, X.; Tao, S. C. Systematic Evaluation of Igg Responses to Sars-Cov-2 Spike Protein-Derived Peptides for Monitoring Covid-19 Patients. *Cell. Mol. Immunol.* **2021**, *18*, 621−631.
(17) Polvere, I.; Voccola, S.; Cardinale, G.; Fumi, M.; Aquila, F.; Parrella, A.; Madera, J. R.; Stilo, R.; Vito, P.; Zotti, T. A Peptide-Based Assay Discriminates Individual Antibody Response to Sars-Cov-2. *Genes Dis.* **2022**, *9*, 275−281.
(18) Simula, E. R.; Manca, M. A.; Jasemi, S.; Uzzau, S.; Rubino, S.; Manchia, P.; Bitti, A.; Palermo, M.; Sechi, L. A. Hcov-Nl63 and Sars-Cov-2 Share Recognized Epitopes by the Humoral Response in Sera of People Collected Pre- and During Cov-2 Pandemic. *Microorganisms* **2020**, *8*, 1993.
(19) Li, Y.; Lai, D. Y.; Zhang, H. N.; Jiang, H. W.; Tian, X.; Ma, M. L.; Qi, H.; Meng, Q. F.; Guo, S. J.; Wu, Y.; Wang, W.; Yang, X.; Shi, D. W.; Dai, J. B.; Ying, T.; Zhou, J.; Tao, S. C. Linear Epitopes of Sars-Cov-2 Spike Protein Elicit Neutralizing Antibodies in Covid-19 Patients. *Cell. Mol. Immunol.* **2020**, *17*, 1095−1097.
(20) Ernst, E.; Wolfe, P.; Stahura, C.; Edwards, K. A. Technical Considerations to Development of Serological Tests for Sars-Cov-2. *Talanta* **2021**, *224*, 121883.
(21) Ayouba, A.; Toure, A.; Butel, C.; Keita, A. K.; Binetruy, F.; Sow, M. S.; Foulongne, V.; Delaporte, E.; Peeters, M. Development of a Sensitive and Specific Serological Assay Based on Luminex Technology for Detection of Antibodies to Zaire Ebola Virus. *J. Clin. Microbiol.* **2017**, *55*, 165−176.
(22) Shrock, E.; Fujimura, E.; Kula, T.; Timms, R. T.; Lee, I. H.; Leng, Y.; Robinson, M. L.; Sie, B. M.; Li, M. Z.; Chen, Y.; Logue, J.; Zuiani, A.; McCulloch, D.; Lelis, F. J. N.; Henson, S.; Monaco, D. R.; Travers, M.; Habibi, S.; Clarke, W. A.; Caturegli, P.; Laeyendecker, O.; Piechocka-Trocha, A.; Li, J. Z.; Khatri, A.; Chu, H. Y.; Collection, M. C.-.; Processing, T.; Villani, A. C.; Kays, K.; Goldberg, M. B.; Hacohen, N.; Filbin, M. R.; Yu, X. G.; Walker, B. D.; Wesemann, D. R.; Larman, H. B.; Lederer, J. A.; Elledge, S. J. Viral Epitope Profiling of Covid-19 Patients Reveals Cross-Reactivity and Correlates of Severity. *Science* **2020**, *370*, No. eabd4250.
(23) Grifoni, A.; Sidney, J.; Zhang, Y.; Scheuermann, R. H.; Peters, B.; Sette, A. A Sequence Homology and Bioinformatic Approach Can Predict Candidate Targets for Immune Responses to Sars-Cov-2. *Cell Host Microbe* **2020**, *27*, 671−680 e2.
(24) Wolfel, R.; Corman, V. M.; Guggemos, W.; Seilmaier, M.; Zange, S.; Muller, M. A.; Niemeyer, D.; Jones, T. C.; Vollmar, P.; Rothe, C.; Hoelscher, M.; Bleicker, T.; Brunink, S.; Schneider, J.; Ehmann, R.; Zwirglmaier, K.; Drosten, C.; Wendtner, C. Virological Assessment of Hospitalized Patients with Covid-2019. *Nature* **2020**, *581*, 465−469.
(25) Grossberg, A. N.; Koza, L. A.; Ledreux, A.; Prusmack, C.; Krishnamurthy, H. K.; Jayaraman, V.; Granholm, A. C.; Linseman, D. A. A Multiplex Chemiluminescent Immunoassay for Serological Profiling of Covid-19-Positive Symptomatic and Asymptomatic Patients. *Nat. Commun.* **2021**, *12*, 740.
(26) Diener, C.; Garza Ramos Martinez, G.; Moreno Blas, D.; Castillo Gonzalez, D. A.; Corzo, G.; Castro-Obregon, S.; Del Rio, G. Effective Design of Multifunctional Peptides by Combining Compatible Functions. *PLoS Comput. Biol.* **2016**, *12*, No. e1004786.
(27) Koppisetti, R. K.; Fulcher, Y. G.; Van Doren, S. R. Fusion Peptide of Sars-Cov-2 Spike Rearranges into a Wedge Inserted in Bilayered Micelles. *J. Am. Chem. Soc.* **2021**, *143*, 13205−13211.
(28) Xu, K.; Acharya, P.; Kong, R.; Cheng, C.; Chuang, G. Y.; Liu, K.; Louder, M. K.; O'Dell, S.; Rawi, R.; Sastry, M.; Shen, C. H.; Zhang, B.; Zhou, T.; Asokan, M.; Bailer, R. T.; Chambers, M.; Chen, X.; Choi, C. W.; Dandey, V. P.; Doria-Rose, N. A.; Druz, A.; Eng, E. T.; Farney, S. K.; Foulds, K. E.; Geng, H.; Georgiev, I. S.; Gorman, J.; Hill, K. R.; Jafari, A. J.; Kwon, Y. D.; Lai, Y. T.; Lemmin, T.; McKee, K.; Ohr, T. Y.; Ou, L.; Peng, D.; Rowshan, A. P.; Sheng, Z.; Todd, J. P.; Tsybovsky, Y.; Viox, E. G.; Wang, Y.; Wei, H.; Yang, Y.; Zhou, A. F.; Chen, R.; Yang, L.; Scorpio, D. G.; McDermott, A. B.; Shapiro, L.; Carragher, B.; Potter, C. S.; Mascola, J. R.; Kwong, P. D. Epitope-Based Vaccine Design Yields Fusion Peptide-Directed Antibodies That Neutralize Diverse Strains of Hiv-1. *Nat. Med.* **2018**, *24*, 857−867.
(29) WHO Tracking Sars-Cov-2 Variants. https://www.who.int/en/activities/tracking-SARS-CoV-2-variants/ (accessed June 24, 2022).
(30) Hodcroft, E. Overview of Variants/Mutations. https://covariants.org/variants (accessed June 24, 2022).
(31) Jumper, J.; Evans, R.; Pritzel, A.; Green, T.; Figurnov, M.; Ronneberger, O.; Tunyasuvunakool, K.; Bates, R.; Zidek, A.; Potapenko, A.; Bridgland, A.; Meyer, C.; Kohl, S. A. A.; Ballard, A. J.; Cowie, A.; Romera-Paredes, B.; Nikolov, S.; Jain, R.; Adler, J.; Back, T.; Petersen, S.; Reiman, D.; Clancy, E.; Zielinski, M.; Steinegger, M.; Pacholska, M.; Berghammer, T.; Bodenstein, S.; Silver, D.; Vinyals, O.; Senior, A. W.; Kavukcuoglu, K.; Kohli, P.; Hassabis, D. Highly Accurate Protein Structure Prediction with Alphafold. *Nature* **2021**, *596*, 583−589.
(32) Mirdita, M.; Schutze, K.; Moriwaki, Y.; Heo, L.; Ovchinnikov, S.; Steinegger, M. Colabfold: Making Protein Folding Accessible to All. *Nat. Methods* **2022**, *19*, 679−682.
(33) Jiang, S.; Hillyer, C.; Du, L. Neutralizing Antibodies against Sars-Cov-2 and Other Human Coronaviruses. *Trends Immunol.* **2020**, *41*, 545.
(34) Min, L.; Sun, Q. Antibodies and Vaccines Target Rbd of Sars-Cov-2. *Front. Mol. Biosci.* **2021**, *8*, 671633.
(35) Yu, F.; Xiang, R.; Deng, X.; Wang, L.; Yu, Z.; Tian, S.; Liang, R.; Li, Y.; Ying, T.; Jiang, S. Receptor-Binding Domain-Specific Human Neutralizing Monoclonal Antibodies against Sars-Cov and Sars-Cov-2. *Signal Transduction Targeted Ther.* **2020**, *5*, 212.
(36) Burbelo, P. D.; Riedo, F. X.; Morishima, C.; Rawlings, S.; Smith, D.; Das, S.; Strich, J. R.; Chertow, D. S.; Davey, R. T.; Cohen, J. I. Sensitivity in Detection of Antibodies to Nucleocapsid and Spike

Proteins of Severe Acute Respiratory Syndrome Coronavirus 2 in Patients with Coronavirus Disease 2019. *J. Infect. Dis.* **2020**, *222*, 206−213.
(37) Wang, P.; Liu, L.; Nair, M. S.; Yin, M. T.; Luo, Y.; Wang, Q.; Yuan, T.; Mori, K.; Solis, A. G.; Yamashita, M.; Garg, A.; Purpura, L. J.; Laracy, J. C.; Yu, J.; Joshua-Tor, L.; Sodroski, J.; Huang, Y.; Ho, D. D. Sars-Cov-2 Neutralizing Antibody Responses Are More Robust in Patients with Severe Disease. *Emerg. Microb. Infect.* **2020**, *9*, 2091−2093.
(38) Ye, Q.; Lu, S.; Corbett, K. D. Structural Basis for Sars-Cov-2 Nucleocapsid Protein Recognition by Single-Domain Antibodies. *Front. Immunol.* **2021**, *12*, 719037.
(39) Cai, X. F.; Chen, J.; Li Hu, J.; Long, Q. X.; Deng, H. J.; Liu, P.; Fan, K.; Liao, P.; Liu, B. Z.; Wu, G. C.; Chen, Y. K.; Li, Z. J.; Wang, K.; Zhang, X. L.; Tian, W. G.; Xiang, J. L.; Du, H. X.; Wang, J.; Hu, Y.; Tang, N.; Lin, Y.; Ren, J. H.; Huang, L. Y.; Wei, J.; Gan, C. Y.; Chen, Y. M.; Gao, Q. Z.; Chen, A. M.; He, C. L.; Wang, D. X.; Hu, P.; Zhou, F. C.; Huang, A. L.; Wang, D. Q. A Peptide-Based Magnetic Chemiluminescence Enzyme Immunoassay for Serological Diagnosis of Coronavirus Disease 2019. *J. Infect. Dis.* **2020**, *222*, 189−193.
(40) Rosadas, C.; Randell, P.; Khan, M.; McClure, M. O.; Tedder, R. S. Testing for Responses to the Wrong Sars-Cov-2 Antigen? *Lancet* **2020**, *396*, No. e23.
(41) Chen, Z.; Zhang, Z.; Zhai, X.; Li, Y.; Lin, L.; Zhao, H.; Bian, L.; Li, P.; Yu, L.; Wu, Y.; Lin, G. Rapid and Sensitive Detection of Anti-Sars-Cov-2 Igg, Using Lanthanide-Doped Nanoparticles-Based Lateral Flow Immunoassay. *Anal. Chem.* **2020**, *92*, 7226−7231.
(42) Alrashoudi, A. A.; Albalawi, H. I.; Aldoukhi, A. H.; Moretti, M.; Bilalis, P.; Abedalthagafi, M.; Hauser, C. A. E. Fabrication of a Lateral Flow Assay for Rapid in-Field Detection of Covid-19 Antibodies Using Additive Manufacturing Printing Technologies. *Int. J. Bioprint.* **2021**, *7*, 399.
(43) Lew, T. T. S.; Aung, K. M. M.; Ow, S. Y.; Amrun, S. N.; Sutarlie, L.; Ng, L. F. P.; Su, X. Epitope-Functionalized Gold Nanoparticles for Rapid and Selective Detection of Sars-Cov-2 Igg Antibodies. *ACS Nano* **2021**, *15*, 12286−12297.
(44) Reddy Chichili, V. P.; Kumar, V.; Sivaraman, J. Linkers in the Structural Biology of Protein-Protein Interactions. *Protein Sci.* **2013**, *22*, 153−167.
(45) Haberland, A.; Muller, J.; Wallukat, G.; Wenzel, K. Antigen-Free Control Wells in an Elisa Set-up for the Determination of Autoantibodies against G Protein-Coupled Receptors-a Requisite for Correct Data Evaluation. *Anal. Bioanal. Chem.* **2018**, *410*, 5101−5105.
(46) Gonzalez-Moa, M. J.; Van Dorst, B.; Lagatie, O.; Verheyen, A.; Stuyver, L.; Biamonte, M. A. Proof-of-Concept Rapid Diagnostic Test for Onchocerciasis: Exploring Peptide Biomarkers and the Use of Gold Nanoshells as Reporter Nanoparticles. *ACS Infect. Dis.* **2018**, *4*, 912−917.
(47) Robin, X.; Turck, N.; Hainard, A.; Tiberti, N.; Lisacek, F.; Sanchez, J. C.; Muller, M. pROC: an open-source package for R and S + to analyze and compare ROC curves. *BMC Bioinf.* **2011**, *12*, 77.
(48) Youden, W. J. Index for Rating Diagnostic Tests. *Cancer* **1950**, *3*, 32−35.
(49) Banach, B. B.; Cerutti, G.; Fahad, A. S.; Shen, C. H.; Oliveira De Souza, M.; Katsamba, P. S.; Tsybovsky, Y.; Wang, P.; Nair, M. S.; Huang, Y.; Francino-Urdaniz, I. M.; Steiner, P. J.; Gutierrez-Gonzalez, M.; Liu, L.; Lopez Acevedo, S. N.; Nazzari, A. F.; Wolfe, J. R.; Luo, Y.; Olia, A. S.; Teng, I. T.; Yu, J.; Zhou, T.; Reddem, E. R.; Bimela, J.; Pan, X.; Madan, B.; Laflin, A. D.; Nimrania, R.; Yuen, K. Y.; Whitehead, T. A.; Ho, D. D.; Kwong, P. D.; Shapiro, L.; DeKosky, B. J. Paired Heavy- and Light-Chain Signatures Contribute to Potent Sars-Cov-2 Neutralization in Public Antibody Responses. *Cell Rep.* **2021**, *37*, 109771.
(50) Cerutti, G.; Guo, Y.; Zhou, T.; Gorman, J.; Lee, M.; Rapp, M.; Reddem, E. R.; Yu, J.; Bahna, F.; Bimela, J.; Huang, Y.; Katsamba, P. S.; Liu, L.; Nair, M. S.; Rawi, R.; Olia, A. S.; Wang, P.; Zhang, B.; Chuang, G. Y.; Ho, D. D.; Sheng, Z.; Kwong, P. D.; Shapiro, L. Potent Sars-Cov-2 Neutralizing Antibodies Directed against Spike N-Terminal Domain Target a Single Supersite. *Cell Host Microbe* **2021**, *29*, 819−833 e7.
(51) Kang, S.; Yang, M.; He, S.; Wang, Y.; Chen, X.; Chen, Y. Q.; Hong, Z.; Liu, J.; Jiang, G.; Chen, Q.; Zhou, Z.; Zhou, Z.; Huang, Z.; Huang, X.; He, H.; Zheng, W.; Liao, H. X.; Xiao, F.; Shan, H.; Chen, S. A Sars-Cov-2 Antibody Curbs Viral Nucleocapsid Protein-Induced Complement Hyperactivation. *Nat. Commun.* **2021**, *12*, 2697.
(52) Tanaka, S.; Olson, C. A.; Barnes, C. O.; Higashide, W.; Gonzalez, M.; Taft, J.; Richardson, A.; Martin-Fernandez, M.; Bogunovic, D.; Gnanapragasam, P. N. P.; Bjorkman, P. J.; Spilman, P.; Niazi, K.; Rabizadeh, S.; Soon-Shiong, P. Rapid Identification of Neutralizing Antibodies against Sars-Cov-2 Variants by Mrna Display. *Cell Rep.* **2022**, *38*, 110348.
(53) Williams, W. B.; Meyerhoff, R. R.; Edwards, R. J.; Li, H.; Manne, K.; Nicely, N. I.; Henderson, R.; Zhou, Y.; Janowska, K.; Mansouri, K.; Gobeil, S.; Evangelous, T.; Hora, B.; Berry, M.; Abuahmad, A. Y.; Sprenz, J.; Deyton, M.; Stalls, V.; Kopp, M.; Hsu, A. L.; Borgnia, M. J.; Stewart-Jones, G. B. E.; Lee, M. S.; Bronkema, N.; Moody, M. A.; Wiehe, K.; Bradley, T.; Alam, S. M.; Parks, R. J.; Foulger, A.; Oguin, T.; Sempowski, G. D.; Bonsignori, M.; LaBranche, C. C.; Montefiori, D. C.; Seaman, M.; Santra, S.; Perfect, J.; Francica, J. R.; Lynn, G. M.; Aussedat, B.; Walkowicz, W. E.; Laga, R.; Kelsoe, G.; Saunders, K. O.; Fera, D.; Kwong, P. D.; Seder, R. A.; Bartesaghi, A.; Shaw, G. M.; Acharya, P.; Haynes, B. F. Fab-Dimerized Glycan-Reactive Antibodies Are a Structural Category of Natural Antibodies. *Cell* **2021**, *184*, 2955−2972 e25.
(54) Gobeil, S. M.; Henderson, R.; Stalls, V.; Janowska, K.; Huang, X.; May, A.; Speakman, M.; Beaudoin, E.; Manne, K.; Li, D.; Parks, R.; Barr, M.; Deyton, M.; Martin, M.; Mansouri, K.; Edwards, R. J.; Eaton, A.; Montefiori, D. C.; Sempowski, G. D.; Saunders, K. O.; Wiehe, K.; Williams, W.; Korber, B.; Haynes, B. F.; Acharya, P. Structural Diversity of the Sars-Cov-2 Omicron Spike. *Mol. Cell* **2022**, *82*, 2050−2068e6.
(55) Brenke, R.; Hall, D. R.; Chuang, G. Y.; Comeau, S. R.; Bohnuud, T.; Beglov, D.; Schueler-Furman, O.; Vajda, S.; Kozakov, D. Application of Asymmetric Statistical Potentials to Antibody-Protein Docking. *Bioinformatics* **2012**, *28*, 2608−2614.
(56) Desta, I. T.; Porter, K. A.; Xia, B.; Kozakov, D.; Vajda, S. Performance and Its Limits in Rigid Body Protein-Protein Docking. *Structure* **2020**, *28*, 1071−1081 e3.
(57) Kozakov, D.; Beglov, D.; Bohnuud, T.; Mottarella, S. E.; Xia, B.; Hall, D. R.; Vajda, S. How Good Is Automated Protein Docking? *Proteins* **2013**, *81*, 2159−2166.
(58) Kozakov, D.; Hall, D. R.; Xia, B.; Porter, K. A.; Padhorny, D.; Yueh, C.; Beglov, D.; Vajda, S. The Cluspro Web Server for Protein-Protein Docking. *Nat. Protoc.* **2017**, *12*, 255−278.
(59) Vajda, S.; Yueh, C.; Beglov, D.; Bohnuud, T.; Mottarella, S. E.; Xia, B.; Hall, D. R.; Kozakov, D. New Additions to the Cluspro Server Motivated by Capri. *Proteins* **2017**, *85*, 435−444.

https://doi.org/10.1021/acsbiomedchemau.3c00010
ACS Bio Med Chem Au 2024, 4, 37−52